Convergent polynomial expansion and scaling in diffraction scattering. II. Convergent polynomial expansion for all energies, slope parameters, and scaling in pp, $\bar{p}p$, $K^{\pm}p$, and $\pi^{\pm}p$ scattering

M. K. Parida

Physics Department, Sambalpur University, Jyoti Vihar-768 017, Orissa, India and Institute of Physics, A/105 Saheed Nagar, Bhubaneswar-751 007, Orissa, India*

(Received 29 November 1977; revised manuscript received 10 May 1978)

Using simple considerations of Mandelstam analyticity of the s plane along with that of the $\cos\theta$ plane by conformal mapping and the convergent polynomial expansion (CPE), a variable $\chi(s,t)$ is constructed which has the potentialities of reproducing some known scaling variables, Regge behavior, and providing information about asymptotic behavior of slope parameters in diffraction scattering of the type $\sim(\ln s)^p$, where $p = 0,1,2$. CPE in terms of Laguerre polynomials in the proposed variable is possible for all energies, but maximum convergence of the series is possible only at asymptotic energies. Use of the first one or two terms in the CPE in χ provides improved fits to the forward slope data at all energies and reasonably good fits to the high-energy slope-parameter data at $|t| = 0.2$ GeV^2, for pp, $\bar{p}p$, $K^{\pm}p$ and $\pi^{\pm}p$ scattering. Information on the asymptotic behavior of slope parameters for these processes is obtained. Data analysis reveals that the strong behaviors in the amplitudes for all these processes cannot be present inside the corresponding figures of convergence in the mapped planes for all energies except near the threshold. A fit to the slope-parameter data for any process determines unknown parameters in the corresponding χ. When the cross-section-ratio data for different processes are plotted against the corresponding χ's all the data for every process starting from $P_{\rm lab} = 3$ GeV/c up to the highest available energy and within the range $|t| \leq |t|_{\rm max}$, where $|t|_{\rm max} = 1.25$, 0.5, 2.0, 1.0, and 1.25 GeV^2 for pp, $\bar{p}p$, K^+p, K^-p, and $\pi^{\pm}p$ scattering, respectively, lie on a scaling curve. For $p_{\rm lab} > 3$ GeV/c data points for $|t| > |t|_{\rm max}$ also approach the scaling curve, and the data for all available values of $|t|$ with $P_{\rm lab} \geq 50$ GeV/c lie on it. For pp scattering it is found that at high energies scaling in the variable χ occurs for larger-$|t|$ data lying well outside the diffraction-peak region. The scaling curves for pp and $\bar{p}p$ scattering are found to be different and those for π^+p and π^-p scattering are found to be very much the same. The scaling curves for K^+p and K^-p scattering are almost the same. Our analysis implies that the data lying on the scaling curves can be represented by CPE in terms of Laguerre polynomials in the variable χ, with the coefficients of expansion independent of energy. The implication of such type of scaling in the data analysis at high energies using CPE is pointed out.

I. INTRODUCTION

Recently many attempts have been made to understand diffraction scattering of hadrons at high energies. Although the dynamics of hadron-hadron interaction are not known, certain systematics have come to light. One of them is the scaling of differential-cross-section ratio. Attempts have been made through geometrical models[1-3] and by means of general principles of axiomatic field theory[4-9] (AFT) to understand scaling phenomena. As a result different types of scaling variables have been proposed. A brief review of works on scaling has been reported in Ref. 10. Scaling variables like $t\sigma_{\rm tot}$ and $ut\sigma_{\rm tot}(s)/[s\sigma_{\rm tot}(s_0)]$ have been proposed by geometrical models.[2,3] Variables like $t(\ln s)^2$, $t\sigma_{\rm tot}^2/\sigma_{\rm el}$, and $tb(s)$ have been predicted[4-9] from exact results based on principles laid down by AFT. Although the exact results predict scaling of the diffraction peak for $s \to \infty$, early onset of scaling in the energy scale starting from laboratory momentum $P_{\rm lab} = 3.65$ GeV/c has been demonstrated in the variable $ut\sigma_{\rm tot}(s)/[s\sigma_{\rm tot}(s_0)]$ by Hamsen and Krisch[2] for small-angle data in pp scattering. Krisch[1,2]-type variables violate the Cerrulus-Martin[11] lower bound for the scattering amplitude.

The significance of scaling in the context of the optimized polynomial expansion[12] (OPE) has been pointed out in Ref. 10. The technique of OPE for scattering amplitudes and form factors developed by Cutkosky and Deo, and Ciulli[12] has proved to be one of the most useful means of getting information on the dynamics of hadronic interactions by analyzing experimental data.[13] Usually OPE for scattering amplitudes involves unknown parameters which depend upon energy. While analyzing the differential-cross-section data one has to determine a set of parameters by a data-fitting procedure for every energy with the help of a computer. Although this program has yielded meaningful results[14] for lower energies, it is definitely cumbersome and may be even untractable for high-energy scattering which involves

a lot of parameters. If, on the other hand, scaling can be shown to be exhibited in OPE in a suitably constructed conformally mapped variable, the scaling function and hence fits to the data at all energies and all angles in the scaling region can be known, once a set of *a priori* unknown parameters in OPE are determined by fitting the experimental data at any single energy in the scaling region. Hence, demonstration of scaling of the data in CPE in a suitable variable χ is important from the point of view of the economic use of computer time in fitting the data by the method of analytic approximations.

Using Mandelstam analyticity of the $x=\cos\theta$ plane and the technique of OPE by conformal mapping, a model of high-energy scattering of hadrons was proposed.[15,16] The images of the cuts formed the boundary of a parabola with focus at the origin and the physical region formed a segment of the right half of the real axis in the mapped plane. The physical region spreads the entire right half of the real axis, the appropriate physical region for Laguerre-polynomial expansion, like $\sim(\ln s)^2$ only in the limit $s\to\infty$. One of the main drawbacks[10] of the conformal transformation proposed in Ref. 16 is that when applied to processes possessing an unsymmetric cut x plane of analyticity it gives rise to spurious cuts in the mapped plane which affect convergence of polynomial expansion. Apart from this and other deficiencies pointed out in Ref. 10 the formula for the slope parameter developed in Ref. 16 suffers from two deficiencies: (i) It could not account for antishrinkage in $\bar{p}p$ scattering, and the shrinkage-antishrinkage pattern in K^-p and $\pi^\pm p$ scattering. (ii) It failed to explain observed increase of slope parameter with energy at high energies in pp, K^+p, and π^+p scattering.

The reason for the deficiency (i) has been attributed[17] to the lack of achieving the correct physical region for all energies and conformal mapping has been developed[17] which achieves the correct physical region for Laguerre-polynomial expansion for all energies, provided that the amplitude possesses one zero at least on the physical region. In this mapping z_1 although the images of the cuts do not form any regular figure of convergence at finite energies, they always stay away from the image of the physical region, allowing for a parabolic figure of convergence for Laguerre-polynomial expansion, and thus CPE exists for all energies. At higher energies the image of the left-hand cut approaches the branches of a limiting parabolic figure of convergence, although the image of the right-hand cut forms the forward portion of the parabola giving a special emphasis of the right-hand cut for scattering near forward angles, much earlier in the energy scale. Thus, CPE goes over to OPE at asymptotic energies. It was shown that the approach from CPE to OPE is faster, the higher the energy is, the closer the position of zero is to the background direction, and the farther the left-hand cut is than the right-hand cut. A universal formula was developed that relates the slope parameter to the equations of boundaries of spectral functions and lines of zeros in the Mandelstam plane. This formula gave a reasonably good description of shrinkage, antishrinkage, and shrinkage-antishrinkage of forward peaks for all the elastic diffraction scattering processes for all energies except for certain objectionable features as described below. The work of Ref. 17 suffers from deficiency (ii) as described above and, in the simplest case of mappings proposed in Ref. 17, two spurious branch points, at $z_1=0$ and $z_1=\infty$, appear, giving rise to a spurious cut which completely overlaps the image of the physical region the the z_1 plane. It has been pointed out that, looked at as a function of x, the conformal transformation z_1 and the representation of Ref. 17 possess no other singularity except the dynamical branch points of the amplitude. Therefore, if one ignores thepossible presence of pole terms, the representation of Ref. 17 conforms to correct analytic properties of the absorptive part. Ciulli[12] has discussed convergence of polynomial expansion in terms of a mapped variable, which introduces an "artificial" cut explicitly along the physical region. In his work,[12] results on the convergence of polynomial expansion have been taken to hold in the presence of an artificial cut along the physical region. Convergence of polynomial expansion for physical values of z_1 may perhaps hold good in the presence of the spurious cut with the $\mathrm{Re}z_1\pm i\epsilon$ prescription above or below the cut. Thus we suppose that the spurious cut causes no problem for convergence as long as it lies on the physical region in the z_1 plane about which the Laguerre-polynomial expansion is made. Also, the simplest conformal mapping used in Ref. 17 introduced a strong behavior at the point $x=-1$, whose image falls inside the figure of convergence in the mapped plane. Further, the capability of CPE developed in Ref. 17 to account for the high-energy slope-parameter data at nonforward angles, on which many data points are now available, had not been tested. In this work we have tried to suggest a remedy for the deficiency (ii) in the work of Ref. 17 along with clarifying the fact that the strong behaviors for all the diffraction scattering processes are present outside or on the corresponding figures of convergence for all energies, except near the threshold, when slope-parameter data at $|t|=0.2$ GeV^2

are also fitted by the formula derived from CPE.

The reason for the deficiency (ii) has been attributed[10] to the lack of inclusion of the s-plane analyticity for pp scattering. When s-plane analyticity is exploited by conformal mapping and OPE along with that of the x plane as adopted in earlier works,[15,16] the formula for the slope parameter accounts for the forward slope data at all energies, including those at ISR energies. This approach yields a variable χ which has the potentialities of reproducing known scaling variables and Regge behavior in the appropriate kinematical region. It has been found[10] that all the available data on the cross-section ratio for pp scattering, starting from $P_{\text{lab}}=50$ GeV/c, approached a scaling curve, when the data were plotted against χ. From the finite lengths of images of the physical region in the z plane it has been argued that the representation of convergent polynomial expansion for different finite energies is not unique, and there is ambiguity and danger in using the asymptotic expansion in terms of Laguerre polynomials at finite energies. In view of the optimal convergence and the fact that the correct physical region for the series expansion is achieved for asymptotic energies, it has been argued that the scaling in χ occurs, as it should, higher in the energy scale. But this type of approach suffers from deficiency (i).

Since deficiency (i) has been successfully removed in Ref. 17, it is interesting to combine with it the use of the s-plane analyticity as it has been adopted in Ref. 10. Since CPE has been developed for all energies in Ref. 17, the possible onset of scaling of the cross-section ratio for different scattering processes much earlier in the energy scale will be further interesting. The scaling of the cross-section ratio in the context of CPE has further importance, as has been pointed out in Ref. 10 and in the second paragraph in this section.

With this idea, using the analyticity of the s plane along with the variable z_1, a variable $\chi = \alpha(s)z_1$ has been constructed that has the potentialities of reproducing some known scaling variables[4,7-9] and Regge behavior in the amplitude for all elastic diffraction scattering processes for $s \gg s_{\text{th}}$ and $|t| \ll t_R$, but the variable becomes $b(s)z_1$ for high energies and all angles. Using the s-plane analyticity by conformal mapping and CPE introduces at most two more parameters than the previous analysis[17] into the formula for slope parameters. In addition, a constant C is used as a free parameter to look into the possible removal of the strong behavior from inside the figure of convergence. Terms up to the first or second in the CPE in χ give a good description of the data for both forward and nonforward slopes for pp, $\bar{p}p$, $K^{\pm}p$, and $\pi^{\pm}p$ scattering, yielding better (in some cases much better) values of χ^2/NDF for forward slopes than those reported in Ref. 17.

The OPE has been used[18] effectively to determine the asymptotic behavior of electromagnetic form factors of proton and pion from data analysis. In the present work, using the s-plane analyticity along with the work of Ref. 17, we obtain information on the asymptotic behavior of slope parameters by analyzing the slope-parameter data. Present analysis reveals that the slope-parameter data on pp scattering cannot distinguish between $\sim\ln s$ or $\sim(\ln s)^2$ type of asymptotic behavior. Although $\bar{p}p$ and K^-p data appear to be approaching constants for large energies, fits to the data are improved when formulas having $\sim(\ln s)^2$ and $\sim(\ln s)$ type of asymptotic behaviors are used for $\bar{p}p$ and K^-p scattering, respectively. Data on $\pi^{\pm}p$ slopes are consistent with $\sim\ln s$ type of asymptotic behavior.

More important is the result in the present work on the early onset of scaling of the cross-section-ratio data for various processes in the corresponding variable χ's. Fits to the forward slope data and the slope parameters at $|t|=0.2$ GeV^2 for different diffraction scattering processes determine the unknown parameters in the corresponding χ's. When the cross-section-ratio data for any of the scattering processes are plotted against the corresponding χ, the data are found to lie on a scaling curve. For every process all the cross-section-ratio data for $P_{\text{lab}} \geq 3$ GeV/c and $|t| \leq |t|_{\max}$, where $|t|_{\max}$ is found to be different for K^+p, K^-p, and $\bar{p}p$ scattering but the same for pp, π^+p, and π^-p scattering, fall on a single curve. As the energy increases from $P_{\text{lab}}=3$ GeV/c, some data for $|t| > |t|_{\max}$ approach to lie on the curve, such that the available data for all $|t|$ and $P_{\text{lab}} \geq 50$ GeV/c lie on the scaling curve. This implies that for a high-energy process, the coefficients in the CPE in χ, for the cross-section-ratio data for all energies with $P_{\text{lab}} \geq 3$ GeV/c and $|t| \leq |t|_{\max}$, are energy independent. Surprisingly, the available high-energy data for pp scattering for larger values of $|t|$ lying well outside the diffraction peak region lie on the same scaling curve. This has been tested for the larger-$|t|$ data at $P_{\text{lab}}=200$ GeV/c and 1500 GeV/c. Recently Cornille[8] has looked into different conditions of scaling and shown that one of the scaling variables at asymptotic energies can be $t\,b(s)$, $b(s)$ being the forward slope parameter. He has defined a class of scaling functions in which are included sums of powers, exponentials, and classical orthogonal polynomials, including Laguerre but excluding Hermite polynomials, with positive coefficients. Our analysis

reveals that a series in Laguerre polynomials in the variable χ, which becomes $tb(s)$ for small $|t|$ and large energies, is possibly a good candidate for scaling function.

Several limitations of the present approach to diffraction scattering have been pointed out in Ref. 10 and Sec. IV of this paper. Scaling in geometrical models has been either assumed[3] or hypothesized.[1,2] But scaling based upon principles of AFT[4-9] is supported by more rigorous theoretical foundations. In the present work, scaling in the variable χ is not proved *a priori* but hypothesized from the uniqueness of CPE at asymptotic energies. Experimental data verify such a hypothesis.

The paper is organized in the following manner. In Sec. II we point out briefly how the s-plane analyticity can be exploited along with that of the x plane by conformal mapping and CPE. In Sec. III data on slope parameters at forward angles and $|t| = 0.2$ GeV^2 are fitted to determine unknown parameters which are relevant regarding strong behavior and for $\chi(s,t)$ as a scaling variable. In this section we get information on the asymptotic behavior of slope parameters for various processes. The success of χ as a scaling variable for various processes is also tested in this section. In Sec. IV we discuss our results and point out possible reasons for early onset of scaling. Limitations of this method are also pointed out in this section.

II. CONFORMAL MAPPING OF THE s AND $\cos\theta$ PLANES

In this section we use Mandelstam analyticity of the s plane for the absorptive part of the amplitude along with that of the $\cos\theta$ plane as developed in Ref. 17 to construct a new variable $\chi(s,t)$. The potentialities of $\chi(s,t)$ as a scaling variable for determining the asymptotic behavior of slope parameters, and the possible existence of a scaling function are discussed. In developing representations for differential cross sections in this section, we assume that scattering near forward angles is due to the absorptive part of the amplitude alone. With this assumption the contribution due to poles has been neglected. There is a host of papers[4-9] which contain such an assumption. It has been shown that the unitarity upper bound for the absorptive part of the amplitude derived by Singh and Roy[5] saturates the high-energy data near forward angles for πN and pp scattering.[5,19] Experimental measurements at high energies show that the real part of the amplitude is small near forward angles for NN, πN, and KN scattering. But away from the forward directions interference between the pole and cut contributions may significantly affect fits to the slope-parameter data. Although in the present and earlier works[10,15,17,18] pole contribution has been neglected, it is important to know how the inclusion of the pole term modifies expressions for the slope parameter for several processes. However, we note that the simple picture of scaling presented subsequently in this paper will be perhaps difficult to realize if pole contributions are explicitly retained. Since, in the present approach pole contributions have not been included, the representations for differential cross section do not possess correct analyticity properties.

In Ref. 17 conformal mapping of the $x = \cos\theta$ plane onto the z_1 plane has been defined as

$$z_1(s,x) = g(x) z_0(s,x) , \tag{1}$$

where

$$g(x) = \frac{(C+x)^2}{[x + x_0(s)]^2} , \tag{2a}$$

$$z_0(s,x) = [\cosh^{-1}\sqrt{\omega_0}]^2 , \tag{2b}$$

with

$$\omega_0(s,x) = \frac{x_- + 1}{x_+ - 1}\,\frac{x_+ - x}{x_- + x} , \tag{2c}$$

x_+ ($-x_-$) being the start of the right- (left-) hand cut in the x plane, and $x = -x_0(s)$ being the position of zero in the backward hemisphere, which, in general, may be energy dependent. With the conformal mapping z_1, the correct physical region for Laguerre-polynomial expansion, $0 \leq \mathrm{Re} z_1 \leq \infty$, is achieved for all energies and the convergent polynomial expansion (CPE) for the differential cross section

$$\frac{d\sigma}{dt} = e^{-\alpha z_1} \sum_n a_n(s) L_n(2\alpha z_1) \tag{3}$$

possesses at least one zero in the physical region. Although the correct physical region has been achieved for all energies and the image of the right-hand cut deviates only slightly from the forward portion of the parabola, the image of the left-hand cut deviates drastically from the branches of the limiting parabola at lower energies. At none of the energies do the images of the branch points touch the image of the physical region. Thus for all energies a parabolic figure of convergence for Laguerre-polynomial expansion exists around the right half of the real axis in the z_1 plane. For any finite energy, however, the interior of the figure of convergence contains only a part of the image of the cut x plane, which increases with energy. As $s \to \infty$, this parabola coincides with the limiting parabola whose forward portion is the image of the right-hand cut and the rest is the image of the left-hand cut, and its in-

terior contains the whole image of the domain of analyticity of the x plane. Thus, according to the established results of Cutkosky and Deo, and Ciulli,[12] the polynomial expansion (3) converges for all energies, the rate of convergence increasing with energy. Only at asymptotic energies is the convergence maximum. In Ref. 10 it has been pointed out that CPE at finite energies in Laguerre polynomials is ambiguous, but convergent expansion in terms of a nonunique set of polynomials is possible and expansion with maximal convergence in Laguerre polynomials is an asymptotic one. In the present work it is clear that expansion in terms of Laguerre polynomials is possible for all energies, the rate of convergence of the series increasing with energy. However, in this case also maximally converging expansion with Laguerre polynomials is an asymptotic expansion.

Since we are stressing analytic representations which converge rapidly, it is important to locate the positions of spurious singularities which may affect analyticity and/or convergence. Regarded as a function of x, the transformation z_1 and the representation (3) possess only branch-point singularities corresponding to dynamical singularities of the absorptive part. But by construction of the mapping $g(x)$, the two-sheeted structure in the y plane, where $y=(c+x)/(x+x_0)$, has been folded together, giving rise to spurious branch points in the $g(x)$ plane at $g(x)=0$ and $g(x)=\infty$. These two branch points appear as square-root branch points in the z_1 plane at $z_1=0$ and $z_1=\infty$. Thus, in the z_1 plane a spurious cut appears, completely overlapping the physical region. Ciulli[12] has discussed convergence of polynomial expansion in terms of a mapped variable which introduces an artificial cut explicitly along the physical region. In his work, results on the convergence properties of the polynomial expansion have been taken to hold in the presence of the artificial cut. Thus we suppose that the spurious cut causes no problem for convergence as long as it lies on the physical region in the z_1 plane about which the Laguerre polynomial expansion is being made. The convergence of polynomial expansion may perhaps hold true for physical values of z_1, with the $\mathrm{Re}z_1 \pm i\epsilon$ prescription above or below the spurious cut.

We now point out the need for exploiting s-plane analyticity to account for the high-energy slope-parameter data. The differential cross section for two-body elastic scattering is a function of two independent variables which we choose as s and $\cos\theta$. The slope parameter at any fixed s is measured by taking a set of data points on the differential cross section at various angles and fitting the data in a given $|t|$ range. Slope parameters at various energies are known by analyzing different sets of differential cross-section data at corresponding energies. Cuts in the s and $\cos\theta$ planes represent forces responsible for the scattering of hadrons. To account for the value of slope at a given energy, the influence of the cut structure in the $\cos\theta$ plane has been exploited by CPE through the variable z_1. But since the slope parameter $b(s,t)$ is also a function of the independent variable s, the cut structure of the abosrptive part of the amplitude in the s plane may drastically influence the behavior of the slope parameter, at least for high energies. The slope parameter $b(s,t)$ is proportional to the parameter α, which, as has been pointed out earlier, is energy dependent.[10,15-17] Other parameters in (3) do not affect the forward slope, although they may affect nonforward slopes. We, therefore, attempt to adopt convergent expansions for $\alpha(s)$. Cutkosky[20] has suggested analytic approximation by the conformal mapping of the individual factors in the corresponding independent variables in a product. For the diffractive process to be considered here, the absorptive part of the forward scattering amplitude has a left-hand cut from $s=s_1$ to $s=-\infty$ where s_1 is determined by the root of the equation $s-\Sigma+t_L=0$, Σ is the sum of the squares of the masses of initial and final particles, and t_L is the equation to the boundary of the spectral function ρ_{su}. The physical region extends along the right half of the real axis starting from threshold value $s=s_{\mathrm{th}}$ to $s=\infty$. In meson-nucleon scattering there are other cuts present in the s plane, but we ignore them since they may not contribute to the absorptive part. Since the physical region is a semi-infinite line, the most suitable conformal mapping of the s plane will be a parabolic transformation onto the $\zeta(s)$ plane

$$\zeta(s)=\eta^2(s)\,, \tag{4a}$$

with

$$\eta(s)=\sinh^{-1}\sqrt{\omega_s}\,, \tag{4b}$$

$$w_s=(s-s_{\mathrm{th}})/(s_{\mathrm{th}}-s_1)\,, \tag{4c}$$

in which the image of the left-hand cut is a parabola with focus at the origin and the image of the physical region is the entire right half of the real axis. In the η plane, however, the left-hand cut is mapped onto the boundary of a strip of width π, but the image of the physical region is also the right half of the real axis. In both cases, the entire domain of analyticity for the absorptive part in the s plane is mapped onto the interior of the figure of convergence in the mapped planes. Thus a series in Laguerre (Hermite) polynomials in $\zeta(s)$ ($\eta(s)$) converges at the fastest rate. But for expansion in terms of $\eta(s)$, the coefficients of the Hermite polynomials are not unambiguously de-

termined, since the correct physical region $-\infty \leq \mathrm{Re}\,\eta \leq \infty$ has not been achieved in this case. This type of mapping with Taylor-series expansion has been used by Deo[21] in the context of virtual compton scattering. We also adopt a convergent Taylor-series expansion in $\zeta(\eta)$. Since most of the slope parameter has been accounted for by mapping of the x plane[17] onto the z_1 plane, we suppose that only a few terms in $\alpha(s)$ are necessary to account for the slope parameter in all the energy ranges. In fact, the unitarity restriction forbids us taking more than the first two (three) terms in the Taylor series in $\zeta(\eta)$. The reason for such a restriction lies in the fact that the maximum growth rate of the slope parameter allowed by unitarity[22] as $s \to \infty$ is $\sim(\ln s)^2$, and $\zeta(s) \underset{s\to\infty}{\to} \sim(\ln s)^2$ and $\eta(s) \underset{s\to\infty}{\to} \sim \ln s$. Thus, the convergent Taylor-series expansion for $\alpha(s)$ can be written as

$$\alpha(s) = \begin{cases} c_0(1 + c_1\zeta), & \text{(5a)} \\ d_0(1 + d_1\eta + d_2\eta^2). & \text{(5b)} \end{cases}$$

From the above expressions we find that the asymptotic behavior of $\alpha(s)$ is of the type $\sim(\ln s)^n$, with $n = 0, 1, 2$. From Ref. 17 and the formulas written in the next section of this paper we see that $\lim_{s\to\infty} b(s, o) = \lim_{s\to\infty} \alpha(s)/(4m_\pi^2)$. Thus, $b(s)$ has the asymptotic behavior $\sim(\ln s)^n$, with $n = 0, 1, 2$, where $n = 0$, 1 corresponds to the constant and Regge types of asymptotic behaviors, respectively, and $n = 2$ corresponds to the saturation of unitarity. Thus, with the use of the s-plane analyticity, the formula for the slope parameter possesses potentialities of saturating some known types of asymptotic behaviors. Now, defining the variable

$$\chi(s, t) = \alpha(s) z_1(s, t), \tag{6}$$

the convergent expansion for the cross-section ratio

$$f(s, t) = \frac{d\sigma}{dt}(s, t) \Big/ \frac{d\sigma}{dt}(s, 0) \tag{7}$$

can be written

$$f(s, t) = \bar{e}^{\chi} \sum_{n=0} e_n L_n(2\chi), \tag{8}$$

where the coefficients e_n's are related to the a_n's of (3) by the relation

$$e_n = \frac{a_n}{\sum_{n=0} a_n L_n(0)} \tag{9}$$

In the expressions (3) and (8) the unknown parameters a_n's and e_n's are, in general, energy dependent. It is possible to take into account the energy dependence of these parameters by some conformal mapping of the s plane. But, while using the conformal-mapping technique to approximate $a_n(s)$ analytically, it may be borne in mind that $a_n(s)$ are "partial-wave amplitudes." It is well known that for unequal-mass scattering the analyticity properties of the partial-wave amplitude are different from the total amplitude. The mapped variable in the present work is different from that in Ref. 10 and thus the analyticity properties of $a_n(s)$ in Eq. (3) of Ref. 10 is different from those of $a_n(s)$ in Eq. (3) in the present work. Since the domains of analyticity for partial-wave amplitudes are not simple, analytic approximations of e_n's and a_n's by conformal mapping may be complicated. But it has been found in Ref. 10 that the use of representation (14) for $f(s, t)$ in terms of χ in that work makes the situation simple for high energies such that in the scaling region one need not worry about the energy dependence of e_n's. Similarly, in this work we will find in the next section that $\chi(s, t)$ is a good scaling variable for the cross-section-ratio data starting even from a few GeV/c of laboratory momentum within a limited $|t|$ range, and all the available data in the very-high-energy region. In effect it will be found that e_n's are energy independent at least in this region.

Before proceeding further we tabulate below certain relevant features of the variable $\chi(s, t)$ and the polynomial expansion (8):

(i) For energies such that $|(4q^2 + t_L - \Delta/s)| \gg |t|$ and angles such that $|t| \ll t_R$, $z_0 \sim -t/t_R$ and the expansion (3) or (8) reproduces the usual exponential fit to the diffraction peak even at low energies. This point was noted in Ref. 17. But for large s and $|t| \ll t_R$, if now we retain terms only up to the second in expansion (5b), $\chi(s, t) \sim t \ln s$ and formula (8) saturates Regge behavior. In general for large energies and small $|t|$, $\chi(s, t) \sim t b(s)$, which is the scaling variable proposed by exact results.[7-9]

(ii) For large energies and $|t| \ll t_R$, if we retain the second (third) term in (5a) [(5b)], $\chi(s, t) \sim t(\ln s)^2$, which is the scaling variable of Auberson, Kinoshita, and Martin.[4]

(iii) From the formula for slope parameters as developed in Ref. 17 and the next section, for large energies the behavior of the forward slope can be written as

$$b(s, o) \underset{s\to\infty}{\to} \frac{\alpha(s)}{4m_\pi^2} = \frac{\chi(s, t)}{4m_\pi^2 z_1}, \tag{10}$$

where relation (6) has been used. Thus, for large energies and all angles,

$$\chi(s, t) = 4m_\pi^2 b(s) z_1. \tag{11}$$

In view of these features of $\chi(s, t)$, it may be potentially useful in describing scaling of $f(s, t)$,

which, according to (8), is possible if the parameters e_n's do not depend upon energy.

In the conformal mapping z_1, a special emphasis has been placed on the influence of the nearest right-hand cut on scattering near forward angles. That the image of the right-hand cut forms the forward portion of the parabola[17] and lies closer to the images of the points near $x=1$ in the mapped plane, takes into account such a feature. The convergence of the series (3) or (8) in the forward direction is further enhanced by the fact that χ (or z_1) $\propto t$, for small $|t|$. In view of these and the more important reason that CPE has been possible at all energies by schieving the correct physical region for all energies,[17] scaling of the small-angle data at least may start earlier in the energy scale. Thus the series expansion (8) may represent small-angle data over a wider range with the same set of e_n's.

Before examining the scaling of the data on $f(s,t)$, it is necessary to known unknown parameters in the variable $\chi(s,t)$ for every process. In the next section we will find that only the forward slope-parameter data cannot help in doing so. In the next section, the universal formulas for slope parameters, both for forward and nonforward angles, are written down using the expansion (8). The fitting of the forward slope-parameter data and the data at $|t|=0.2$ GeV^2 is carried out to test the improvement caused due to the use of s-plane analyticity, to get information on asymptotic behaviors of slope parameters for several processes, and to determine the unknown parameters in χ. The value of C determined in this way supplies information about the position of the point where strong behavior of the amplitude lies in the mapped plane.

III. SLOPE PARAMETERS AND SCALING OF THE CROSS-SECTION RATIO

In this section we first examine how the use of the s-plane analyticity in CPE, as discussed in the previous section, improves the fit to the slope-parameter data and supplies information on the asymptotic behavior of slope parameters. We will see that to know all the parameters in $\chi(s,t)$, it is necessary to fit the forward as well as nonforward slope data. We report fits to the data with the corresponding χ^2/NDF values for forward slopes and the slope parameters at $|t|=0.2$ GeV^2 for pp, $\bar{p}p$, $K^{\pm}p$, and $\pi^{\pm}p$ scattering. Among the unknown parameters in $\chi(s,t)$, the value of C which occurs in (2a), implies that the strong behavior for all these processes cannot occur inside the figure of convergence in the mapped plane for all energies except for the case $s \to s_{\text{th}}$. To look into the efficiency of $\chi(s,t)$ as a scaling variable and possible onset of scaling earlier in the energy scale, data on $f(s,t)$ are plotted against χ for different processes.

The slope parameter $b(s,t)$ can be defined as

$$b(s,t)=\frac{d}{dt}\ln f(s,t). \tag{12}$$

It has been already remarked that, for large energies and small angles, $z_1 \propto t$. In this kinematical region the convergence of series (3) or (8), in addition to being accelerated by conformal mapping, is further accelerated by virtue of the variables being proportional to t. We, therefore, suppose that only the first term (two terms) in the expansion (8) may be necessary for describing the slope parameter at $|t|=0$ ($|t|_{\text{av}}=0.2$ GeV^2), with

$$b(s,0)=-\left.\frac{d\chi}{dt}\right|_{t=0}=\frac{4q^4\alpha(s)(C+1)^2}{F^2(s,0)}\,\frac{1}{t_R}\left(1+\frac{t_R}{4q^2+t_L-\Delta/s}\right) \tag{13}$$

$$\begin{aligned} b(s,t)&=-\frac{d\chi}{dt}+\frac{d}{dt}\ln[e_0+e_1(1-2\chi)] \\ &=\alpha(s)\frac{[2q^2(C+1)+t]}{F^2(s,t)}\left\{\frac{[2q^2(C+1)+t]}{t_R}\left(1+\frac{t_R-t}{4q^2+t_L-\Delta/s+t}\right)\frac{\sqrt{z_0}}{[w_0(w_0-1)]^{1/2}}\right. \\ &\quad\left.-2\left[1-\frac{2q^2(C+1)+t}{F(s,t)}\right]z_0\right\}\left(\frac{1+2a(\chi-1)}{1+2a\chi}\right), \end{aligned} \tag{14}$$

where

$$F(s,t)=4q^2+u_0(s)-\Delta/s+t\ , \tag{15}$$

$u_0(s)$ being the value of u on the line of zero, and $a=-e_1/(e_0+e_1)$. It can be easily verified that Eq. (13) is obtained from (14) by putting $t=0$ and $a=0$. From (13) it is clear that only the forward slope-parameter data cannot determine C and $\alpha(s)$ simultaneously. We therefore use the data on forward and nonforward slopes at $|t|=0.2$ GeV^2 to determine

these parameters, which in turn determine $\chi(s,t)$. Since $b(s) \propto \alpha(s)$, retaining terms up to the first, second, and third in Eq. (5b) yields asymptotic behaviors of the type ~const, ~ln$s$, and ~$(\ln s)^2$ for the slope parameter. Thus, formulas (13)–(15), along with (5a) and (5b) have the potentialities of verifying the asymptotic behaviors of slope parameters from experimental data. We will use these formulas for data analysis for pp, $\bar{p}p$, $K^{\pm}p$, and $\pi^{\pm}p$ scattering.

A. pp scattering

Experimental data on forward slopes for high-energy pp scattering[23,24] show a ~ln$s$ type of increase consistent with the exchange of a Pomeron of slope $\alpha'(0) = 0.28\ \mathrm{GeV}^{-2}$. Formulas developed in earlier works[16,17] yielded a constant value of slope for $s \to \infty$. The analyticity of the s plane has been exploited[10] to good effect to fit such a shrinkage pattern and exhibit scaling in the cross-section-ratio data at high energies. In Ref. 10 however, the average data of Hansen and Krisch[2] have been used for the purpose of data fitting evaluating unknown parameters in χ. In the context of the theory of analytic approximation for diffraction scattering, no formula has yet been proposed which yields a good χ^2/NDF both for forward slopes and the slope parameter at $|t| = 0.2\ \mathrm{GeV}^2$, on which many points are now available.[25,26] We find that using the general formulas (13) and (14) along with (5a) or (5b) gives good χ^2/NDF for the actual forward and nonforward slope data at all energies. In Ref. 17, the Krisch[1] type of line of zero, as suggested by the analysis of Odorico,[27] was used for data fitting with

$$u_0(s) = -2q^2 + (4q^4 - as)^{1/2}\,. \tag{16}$$

Such zeros, however, introduce spurious branch points in the amplitude at

$$s = s_{\pm} = 4m^2 \pm 2(4m^2 a + a^2)^{1/2} \tag{17}$$

which affect analyticity in s and the optimal convergence of expansion (5) since, due to their presence, the size of the figure of convergence is limited in the $\zeta(\eta)$ plane. Although these branch points spoil the optimality of convergence, the expansions (5) are definitely more convergent than would have been the case otherwise, without conformal mapping. In spite of these limitations introduced by the Krisch[1] type of line of zero, we will use it for fitting the pp data for the sake of convenience and in the absence of any other definite results. With this line of zero we have, for pp scattering,

$$F(s,t) = 2q^2 + (4q^4 - as)^{1/2} + t \tag{18}$$

For data fitting we have chosen 58 data points[23,24] for forward slopes at all available energy ranges whose average value of $|t|$ ($|t|_{\mathrm{av}}$) was less than 0.1, and 25 data points[23–25] for which $|t|_{\mathrm{av}} = 0.2\ \mathrm{GeV}^2$. Using formulas (5a), (13), (14), and (18), a three parameter fit to all these data points are obtained with

$$\begin{aligned} c_0 &= 0.356\,, \\ c_1 &= 0.0089\,, \\ C &= 1.913\,. \end{aligned} \tag{19}$$

For this fit we took $a = 0$ and the equation for $t_{R_{pp}} = t_{L_{pp}}$ was taken to be the elastic boundary ρ_{st}. Adding a as a free parameter does not improve the fit. For this fit the value of χ^2/NDF was found to be 1.83 (0.78) for forward (nonforward) slopes. In view of our use of the actual data points, this value is quite good. Except for the fit of Hansen and Krisch,[2] in which the average of the data had been used, ours is the first fit which reports such a low value of χ^2/NDF for the actual data for forward and nonforward slopes. In Ref. 17 the best fit yielded a χ^2/NDF = 14.9. Although such a large value was partly due to mixing of data for larger $|t|_{\mathrm{av}}$ in the fit, the main reason was the inability of the formula to account for the increasing value of the slope parameter for increasing s in the CERN ISR energy region. In the present formula the inclusion of the s-plane analyticity by conformal mapping has remedied such a deficiency and drastically improved the fit. This fit to the data points has been shown in Fig. 1. Visually, the fit appears very good for all the data. In Ref. 10 an effective boundary of spectral function which retreats away from the theoretical boundary for lower energies was needed to fit the data at all energies. But in the present work a good fit to the data for all energies has been achieved with the theoretical boundary.

We next tried to fit the same data with the expression for $\alpha(s)$ given by (5b), but other expressions remaining unchanged. A three-parameter fit is obtained with

$$\begin{aligned} d_0 &= 0.287\,, \\ d_1 &= 0.102\,, \\ C &= 1.917\,, \end{aligned} \tag{20}$$

for which χ^2/NDF = 1.84 (0.72) for forward (nonforward) slopes. In this case, the addition of the parameters d_2 and a_1 does not improve the fit. The fit is almost the same as that given by (19). Thus, the present data are unable to distinguish between the ~ln$s$ or ~$(\ln s)^2$ type of asymptotic behavior of the slope parameter. The value of C now pushes the strong behavior of the amplitude to the

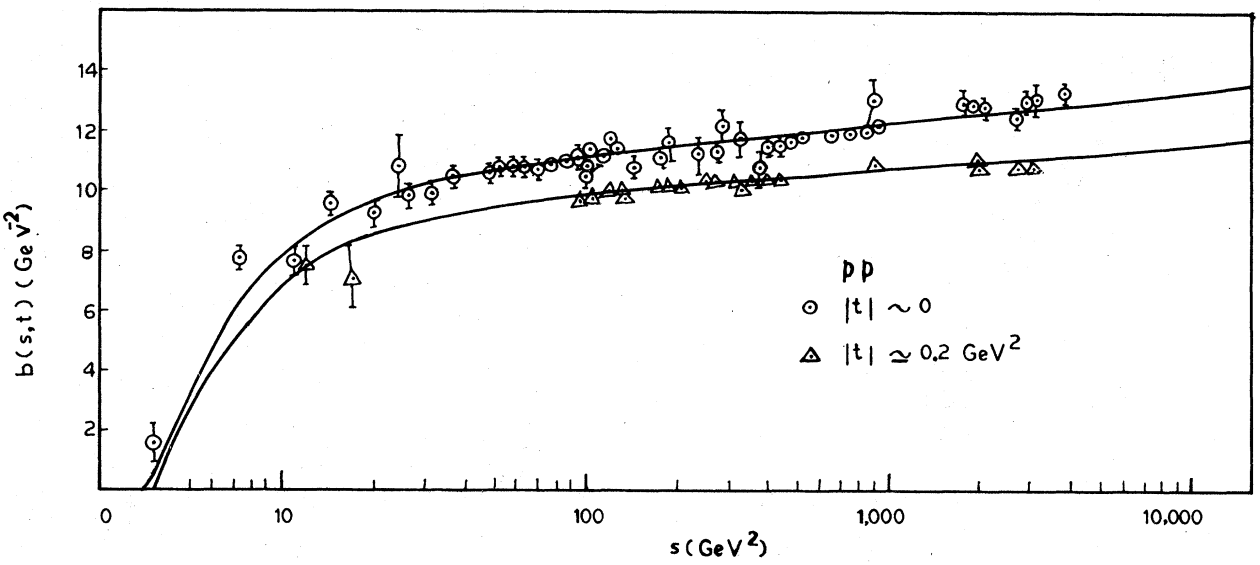

FIG. 1. Fit to the slope-parameter data of pp scattering. The circles are the slope-parameter data near forward angles and the triangles are the data for $|t| = 0.2$ GeV^2. The solid lines indicate our fit.

point $x = -1.917$ lying on the left-hand cut for all values of energy except for $q^2 \to 0$. Thus, its image lies outside the figure of convergence in the mapped plane for all values of energy, except for very low energies near threshold. For $s \to \infty$ this point lies on the limiting parabola. The unknown parameters in χ now being determined by fits to the slope-parameter data, we plot the cross-section-ratio data[25,26,28,29] $f(s,t)$ against χ to see if there is scaling. Figure 2 shows such a plot for small-angle data with $|t| \leq 1.25$ GeV^2 and for all energies starting from $P_{\text{lab}} = 3$ GeV/c. It may be noted that, as compared to the scaling plots Fig. 2 of Ref. 10 and Fig. 5 of Hansen and Krisch,[2] this plot has an expanded vertical scale. Also, the present plot in Fig. 2 covers a larger range of $|t|$ as compared to that of Hansen and Krisch.[2] From Fig. 2 it appears that larger-angle data for $P_{\text{lab}} = 3$–6 GeV/c deviate slightly from the scaling curve, but, if plotted in the same scale as that of Ref. 2 and Ref. 10, all the data of Fig. 2 would appear to lie on the same scaling curve. Figure 3(a) shows the plot of still-larger-angle data for several energies with $|t| > 1$ GeV^2. It is clear that data for lower energies and for larger angles deviate away from the scaling curve. But, as energy increases, the data for larger values of $|t|$ tend to lie on the scaling curve. Figure 3(b) shows that all the larger-$|t|$ data starting from $P_{\text{lab}} = 50$ GeV/c up to $P_{\text{lab}} = 1500$ GeV/c fall on the same curve. Surprisingly, we find that all the available data,[29] even for large $|t|$ values up to $|t| \simeq 10$ GeV^2 for $P_{\text{lab}} = 200$ GeV/c, from Akerlof *et al.*[29] and Hartmann *et al.*,[29] and $P_{\text{lab}} = 1500$ GeV/c from De Kerret *et al.*,[29] fall on the same curve. So far, no variable has been tested to scale the larger-$|t|$ data in such a remarkable fashion. We find that scaling in the small-angle region starting from $P_{\text{lab}} = 3$ GeV/c is at least of the same type as that of Hansen and Krisch.[2] Whereas scaling in the variable of Hansen and Krisch has been plotted for a small-$|t|$ range, the present plot of Fig. 2 covers a larger-$|t|$ range in the small-angle region. The present scaling for small-angle data is much better than those observed in the geometrical scaling variable[3,29] $t\sigma_{\text{tot}}$, which has been already tested[2] to be a bad scaling variable even for small-angle data (Figs. 5 and 6 of Ref. 2) and the variable $t\sigma_{\text{tot}}^2/\sigma_{\text{el}}$ as observed in the work of Divakaran and Gangal.[6] It has been remarked by Hansen and Krisch[2] and noted by Giacomelli[30] that energy dependence is not removed for the larger-angle data. Divakaran and Gangal[6] have noted that scaling in the variable $t\sigma_{\text{tot}}^2/\sigma_{\text{el}}$ becomes worse for larger-angle data. But, in the present work, scaling in the variable χ is remarkably well exhibited for all the available data both for smaller and larger angles starting from $P_{\text{lab}} = 50$ GeV/c. The scaling in χ determined by the fit (19) also yields the same type of result.

B. $\bar{p}p$ scattering

As has been discussed in Ref. 17, the lower-energy data are better fitted with a curve line of

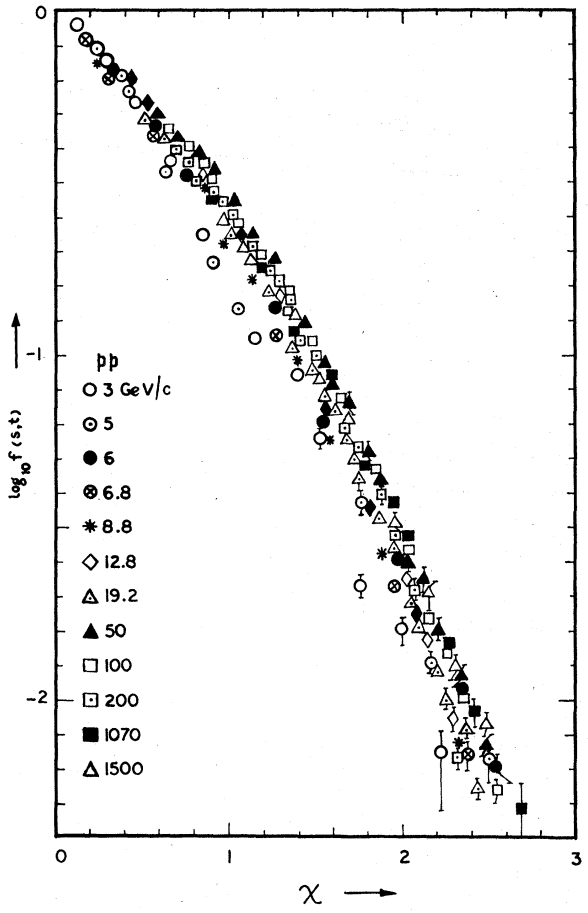

FIG. 2. Scaling and approach to scaling for pp scattering for small-angle data. Quantitites inside the figure indicate P_{lab} (GeV/c).

zeros

$$(s-u_1)[u_0(s)-u_1]=C_2 \tag{21}$$

for which

$$F(s,t)=4q^2+u_1+\frac{C_2}{s-u_1}+t\ , \tag{22}$$

and with elastic boundaries of ρ_{st} (ρ_{su}) for $t_{R\bar{p}p}$ ($t_{L\bar{p}p}$). We have taken[23,25,26,31,32] 44 data points for which $|t|_{\text{av}} \leq 0.11$ GeV^2 to be the forward slope data and 23 data points[23,25,26,31] for $|t|_{\text{av}}=0.2$ GeV^2. With the formulas (13), (14), (22), and (5b), we first tried to fit the data with $d_1=d_2=0$, a choice corresponding to $\lim_{s\to\infty} b(s) \to$ const apparently consistent with experimental data and adopted in Ref. 17. The best-fit values of parameters in this case are

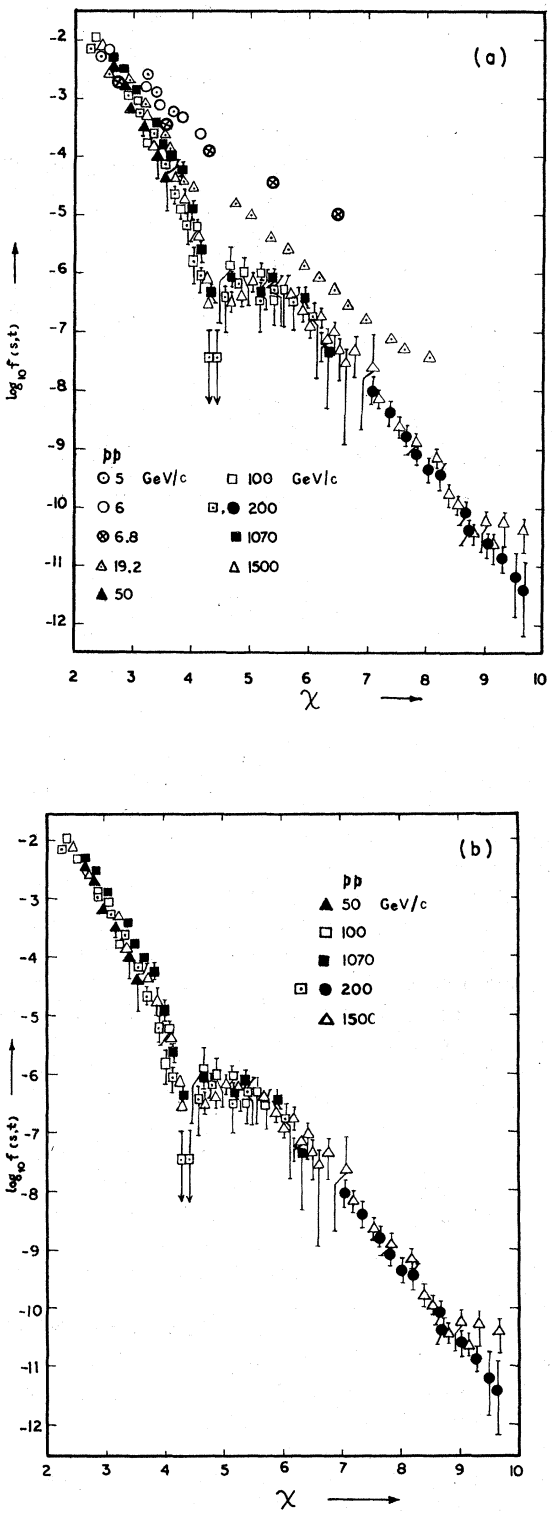

FIG. 3. Scaling and approach to scaling for pp scattering for (a) larger-angle data (b) larger-angle data for high energies only.

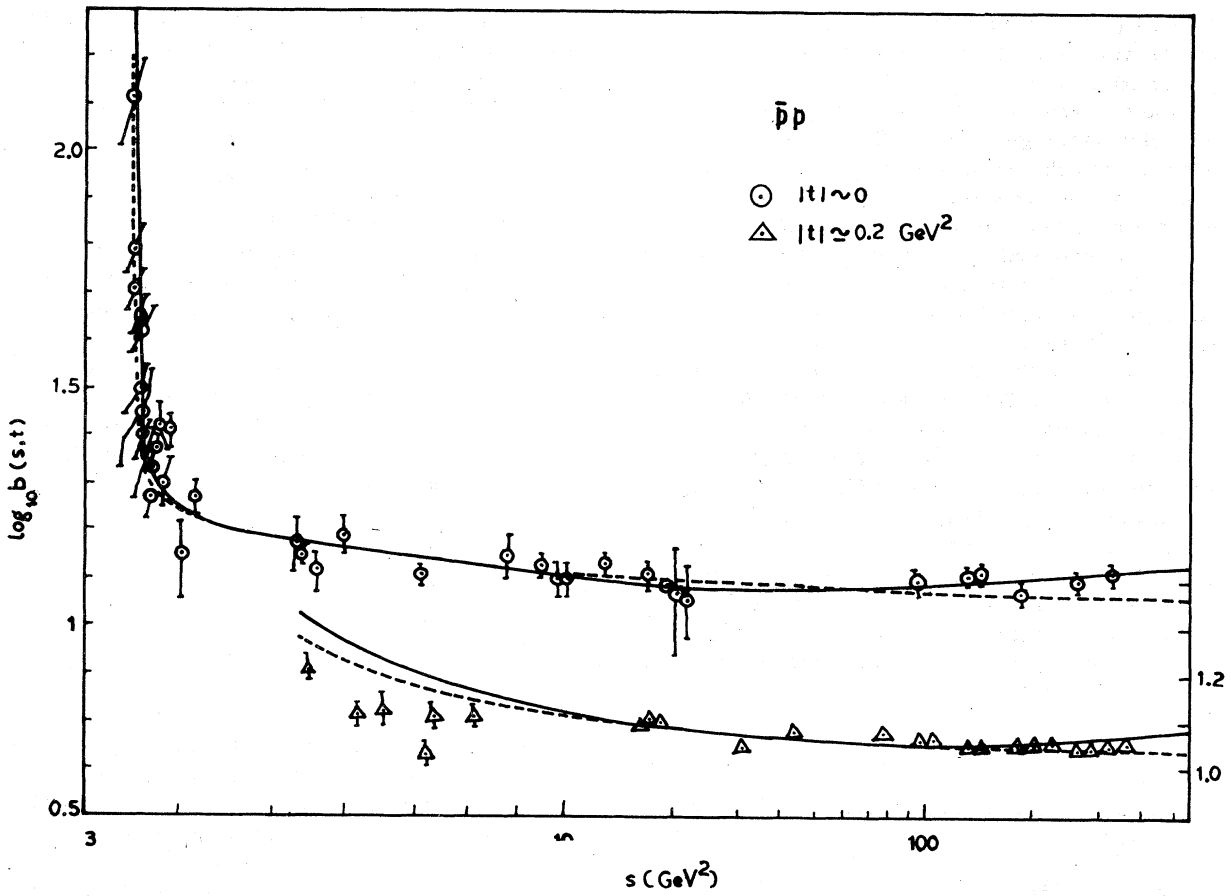

FIG. 4. Fit to the slope-parameter data for $\bar{p}p$ scattering. Circles denote data points near forward angles and triangles are the data points at $|t| = 0.2$ GeV^2, for which the vertical scale is shown at the right of the figure. The dotted (solid) lines correspond to constant $[(\ln s)^2]$ type of asymptotic behavior.

$$
\begin{aligned}
&d_0 = 0.4137, \\
&C_2 = 2.788 \text{ GeV}^4, \\
&u_1 = -0.687 \text{ GeV}^2, \\
&C = 1.9613, \\
&a = -0.0196.
\end{aligned}
\tag{23}
$$

For this fit, $\chi^2/\text{NDF} = 7.5$ (7.9) for forward (nonforward) slopes. This fit has been shown by the dotted curve in Fig. 4. Although almost the same χ^2/NDF for forward slopes has been obtained with the same formula, as in Ref. 17, the significance of the present fit is the inclusion of accurate data[26] on forward and nonforward slopes for high energies, which was not included previously, and the choice of C as a free parameter. The value of C in (23) reveals that the strong behavior lies outside or on the figure of convergence, as in pp scattering, for all energies except for $q^2 \to 0$. As $s \to \infty$, of course, the strong behavior lies on the limiting parabola. To see if the inclusion of s-plane analyticity improves the fit, we first tried formula (5b) with $d_2 = 0$. This choice did not improve the fit. We next included d_1 and d_2 together as free parameters with the idea that possibly the negative value of d_1 and the positive value of d_2 may account for shrinkage-antishrinkage at high energies in a more effective manner. The best-fit values of the parameters are

$$
\begin{aligned}
&d_0 = 0.3339, \\
&d_1 = -0.1173, \\
&d_2 = 0.0459, \\
&C_2 = 2.793 \text{ GeV}^4, \\
&u_1 = -0.687 \text{ GeV}^2, \\
&C = 2.403, \\
&a = 5.913.
\end{aligned}
\tag{24}
$$

This fit yields $\chi^2/\mathrm{NDF}=3.98$ (18.4) for forward (nonforward) slopes with two more parameters as compared to the fit (23). In this case the fit for the forward (nonforward) slope has improved (deteriorated) significantly. This fit suggests asymptotic behavior of the type $\sim(\ln s)^2$ and has been shown by the solid curves in Fig. 4. It is clear that inclusion of the s-plane analyticity by conformal mapping has improved the fit for forward slopes. The fit for nonforward slopes may perhaps be improved by including other parameters in the theory.

The values of the unknown parameters in χ being determined as in (24), we now plot the data[25,26,32] on $f(s,t)$ against $\chi(s,t)$ for $\bar{p}p$ scattering. Figure 5 shows such a plot for smaller $|t|$ data for all energies starting from $P_{\mathrm{lab}}=3$ GeV/c. It is clear that all the data points lie on the scaling curve. High-energy data points for larger values of $|t|$ are not adequate to exhibit some definite conclusions on scaling, but we have found the same trend as observed for large-angle data on pp scattering. Larger-$|t|$ data at lower energies deviate from the scaling curve. As the energy increases, data for larger and larger values of $|t|$ tend to lie on the scaling curve. However, all the data points lying within $|t|\leq 0.5$ GeV^2 for $P_{\mathrm{lab}}=3$–200 GeV/c fall on the same scaling curve.

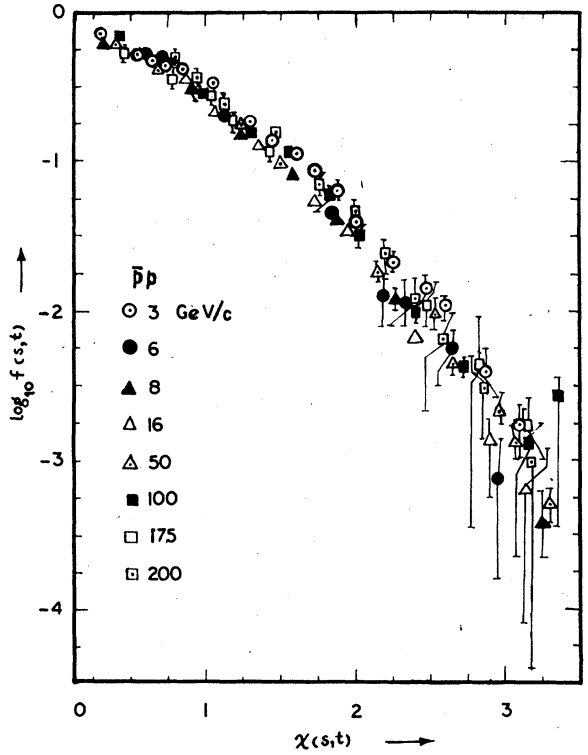

FIG. 5. Scaling and approach to scaling in $\bar{p}p$ scattering.

C. K^+p scattering

We have chosen[23,25,26] 56 data points in all energy ranges with small $|t|_{\mathrm{av}}$ as the forward slope parameters for data fitting. We have also taken 13 data points[25,26] at $|t|_{\mathrm{av}}=0.2$ GeV^2. A fixed-u line of zero with $u_0(s)=$const, theoretical elastic boundaries, ρ_{st} for t_{RK^+p}, and an assumed shape[16,17] for t_{LK^+} were taken to fit the data on K^+p slopes. Using these in formulas (13)–(15), and the expression (5b) for $\alpha(s)$ we obtain the best fit to the data with 4 parameters,

$$\begin{aligned} &d_0=0.1594,\\ &d_1=0.958\\ &u_0(s)=0.3272\ \mathrm{GeV}^2,\\ &C=1.974. \end{aligned} \tag{25}$$

This fit yields a $\chi^2/\mathrm{NDF}=1.09$ as compared to 15.9 in earlier analysis.[17] Although a small part of the improvement of the value of χ^2/NDF is due to the choice of the small-$|t|$ data, this analysis demonstrates the significant improvement due to inclusion of the s-plane analyticity. For the slope-parameter data at $|t|_{\mathrm{av}}=0.2$ GeV^2, this fit yields $\chi^2/\mathrm{NDF}=3.9$. The fit suggests asymptotic behavior of the type $\sim\ln s$ and has been shown by the solid curves in Fig. 6. Addition of a and d_2 as free parameters did not improve the fit and their values were consistent with zero. The value $C=1.974$ implies that the strong behavior lies outside or on the figure of convergence in the mapped plane for all energies except near threshold. At asymptotic energies the location of the strong behavior occurs on the figure of convergence.

The unknown parameters in $\chi(s,t)$ now being known, we plot the data[24,26] on $f(s,t)$ against χ. Figure 7 shows the plot of all the data lying within $|t|\leq 2.0$ GeV^2 for $P_{\mathrm{lab}}\geq 3$ GeV/c. The spread in Fig. 7 is due to the fact that K^-p data in this range have also been plotted in the same curve, as will be described shortly in this section. It is very clear that all the available data in this angular range lie on the same scaling curve. For still larger values of $|t|$, the data points are not adequate for very high energies to draw some definite conclusion from graph plotting. But there is a clear trend showing that larger $|t|$ data for lower energies deviate from the scaling curve and as energy increases from $P_{\mathrm{lab}}=3$ GeV/c, data for larger values of $|t|$ tend to lie on the scaling curve. All

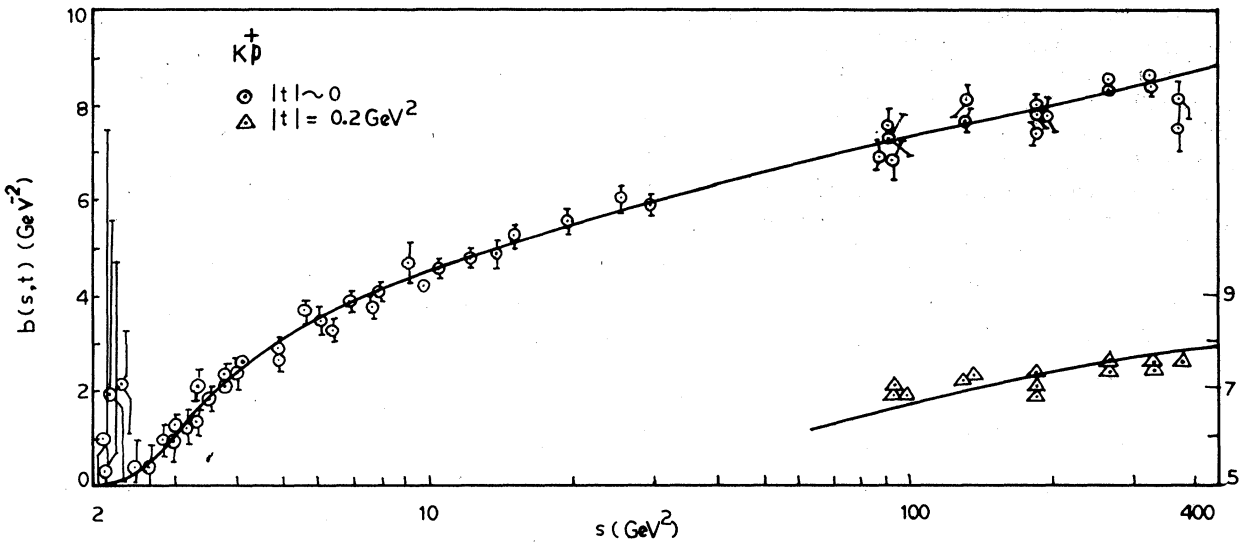

FIG. 6. Fit to the slope-parameter data for K^+p scattering. Circles denote data near forward angles, but the triangles denote data for $|t| = 0.2$ GeV^2 for which the vertical scale is shown on the right-hand side of the figure. Solid lines denote our fits.

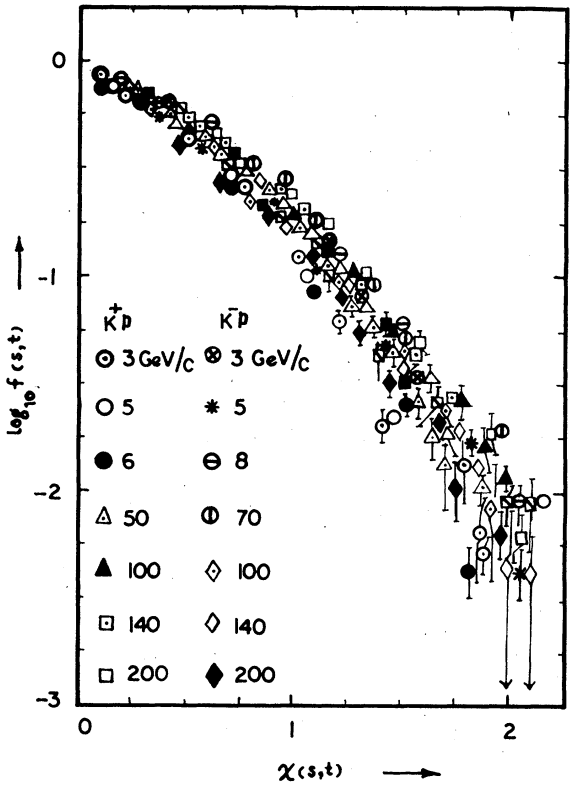

FIG. 7. Scaling and approach to scaling in $K^\pm p$ scattering. ing. The spread for larger $|t|$ is due to the fact that scaling curves for the two processes are not exactly the same.

the available data for $P_{lab} \geq 50$ GeV/c lie on the scaling curve.

D. K^-p scattering

The available data on forward slopes[23,25,26] for this process are quite erratic and oscillate very rapidly at low energies. As has been pointed out in Ref. 17, the only theoretical formula which has given a good fit to the oscillatory pattern on the data is due to Barger and Cline.[33] But this work has been strongly criticized by Weare[34] who has pointed out that the range of energy in which the theory should work is much larger than the authors[33] have used in their calculation, and that there is not even a qualitative explanation of the shrinkage-antishrinkage pattern at lower and intermediate energies. Our formula[17] is free of this type of criticism and the analysis of Ref. 17 with formulas (13) and (15), fixed-u lines of zero, and $\alpha(s) = \text{const}$ yielded oscillations in the low-energy region. This is due to the overlapping boundary structure in ρ_{st} which is related to the slope-parameter formula. Regarding oscillations, we do not expect better results from the present formula. Because of the inherent inability of the formulas to match rapid oscillations in the data, the oscillatory pattern of the data below $s = 2.5$ GeV^2 is avoided with the supposition that their large contributions to the χ^2 value might obscure true information about the use of s-plane analyticity. For data analysis we use 122 data points[23,25,26] for

small $|t|$ values as forward slopes in all available energy ranges with $s \geq 2.5$ GeV^2, including those from Refs. 25 and 26 which were not included earlier,[17] and 22 data[25,26,32] points at high energies for $|t|_{av} = 0.2$ GeV^2. We use the same type of formula as in K^+p scattering except for the fact that for t_{RK^-p} we use the effective shape as described in Ref. 17. The best-fit values of the parameters are

$$\begin{aligned} &d_0 = 0.3731, \\ &d_1 = 0.0146, \\ &u_0(s) = 0.0129 \text{ GeV}^2, \\ &C = 1.505, \\ &a = -0.1397, \\ &\lambda = 0.070 \text{ GeV}, \end{aligned} \tag{26}$$

which yields a χ^2/NDF value 4.83 (9.45) for forward (nonforward) slopes. This fit suggests asymptotic behavior like ~ln$s$ and is shown by the solid curves in Fig. 8. Using other possible combinations of parameters did not improve the fit and the values of other parameters introduced were consistent with zero. The fit to the forward slope has been extrapolated to the lower-energy region in which the data points are denoted by solid circles and were not taken for χ^2 fit. It is clear that the oscillation of the slope parameter is beautifully retained. It is clear that our formula gives a good description of the average of the data in all energy ranges. The strong behavior in this case also lies outside the figure of convergence for all energies except for $q^2 \to 0$, although it lies on the figure of convergence for $s \to \infty$. From the value of λ obtained from data analysis, we observe that the fit to the data requires an effective shape of spectral function which yields the domain of analyticity somewhat smaller than the theoretical one for the absorptive part of the amplitude at lower energies. We have tried a fit by chosing the theoretical value $\lambda = m_\pi$ and varying other parameters. In that case there is almost no change in the fit of Fig. 8 for higher energies, although there is a change at lower energies. But such a change in the fit at lower energies does not affect our results on scaling discussed below.

The unknown parameters in χ being thus determined, we now plot the data[25,26,32] on $f(s,t)$ against

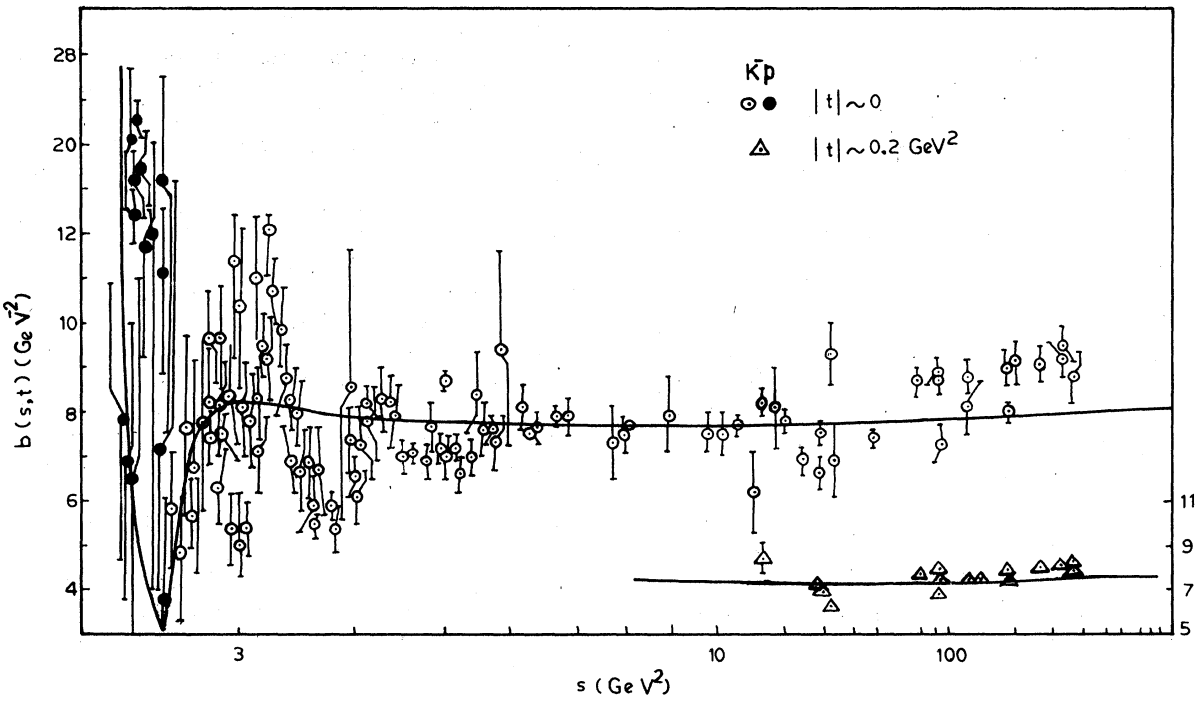

FIG. 8. Fit to the slope-parameter data for K^-p scattering. Open circles denote data near forward angles which were taken for the fit and the triangles denote the data for $|t| = 0.2$ GeV^2 for which the vertical scale is shown at the right-hand side of the figure. Closed circles denote data points at a lower-energy region which were not taken for the fit. The solid lines indicate our fits.

χ in Fig. 7, where scaling for K^+p scattering has also been displayed. This is done with the intention of studying whether the data of K^-p scattering scale individually or in a combined fashion with that of K^+p scattering. It is clear that the data on K^+p and K^-p scale individually and also in combination in the corresponding χ's. In the case of K^-p scattering, all the data for $|t| \leq 1$ GeV^2 and starting from $P_{\rm lab} = 3$ GeV/c onwards, lie on the scaling curve. As energy increases, data for larger $|t|$ approach to lie on the curve. The data for smaller $P_{\rm lab}$ and larger $|t|$ tend to deviate from the scaling curve.

E. $\pi^\pm p$ scattering

For $\pi^\pm p$ scattering we use fixed-u lines of zero, elastic boundaries for $t_{L_{\pi^\pm p}}$, and effective boundaries for $t_{R_{\pi^\pm p}}$ as described in Ref. 17, along with the formulas (13)–(15) and (5b) for data analysis. In these cases we also avoid rapidly oscillating data[22] below $s = 5$ GeV^2 for π^+p scattering, and $s = 4$ GeV^2 for π^-p scattering. Use of fixed-u lines of zero introduces infinities as seen in Ref. 17, but the infinities can be avoided by using curved line of zero.[17] Both the types of lines of zero yield almost the same fit for the high-energy region.[17] For this reason we test the impact of the use of s-plane analyticity on data analysis by using only the fixed-u lines of zeros.

(i) π^+p scattering

For π^+p scattering the best-fit values of the parameters are

$$\begin{aligned} &d_0 = 0.4010\,, \\ &d_1 = 0.1102\,, \\ &u_0(s) = 0.2904 \text{ GeV}^2\,, \\ &C = 1.2112\,, \\ &a = -0.1875\,, \\ &\lambda = 0.184 \text{ GeV}\,. \end{aligned} \tag{27}$$

For this fit, 52 data points for forward slopes[23,25,26] and 16 data points[23,25] for the slope parameter at $|t|_{\rm av} = 0.2$ GeV^2 were taken. The value of χ^2/NDF for the fit is 3.75 (26.3) for forward (nonforward) slopes. The contribution to the χ^2 value due to four data points for nonforward slopes is 336 out of the total 369. The value of C indicates that the strong behavior is removed from the interior of the figure of convergence for all practical purposes except for $q^2 \to 0$, although it lies closer to the origin than those in pp, $\bar{p}p$, and $K^\pm p$ scattering. The fit has been shown by the solid curves in Fig. 9. We find that it is difficult to reconcile the forward slope data of Foley *et al.*,[28] in the range $12 \leq s \leq 40$ GeV^2 with other data points at higher and lower energies. It has been concluded by

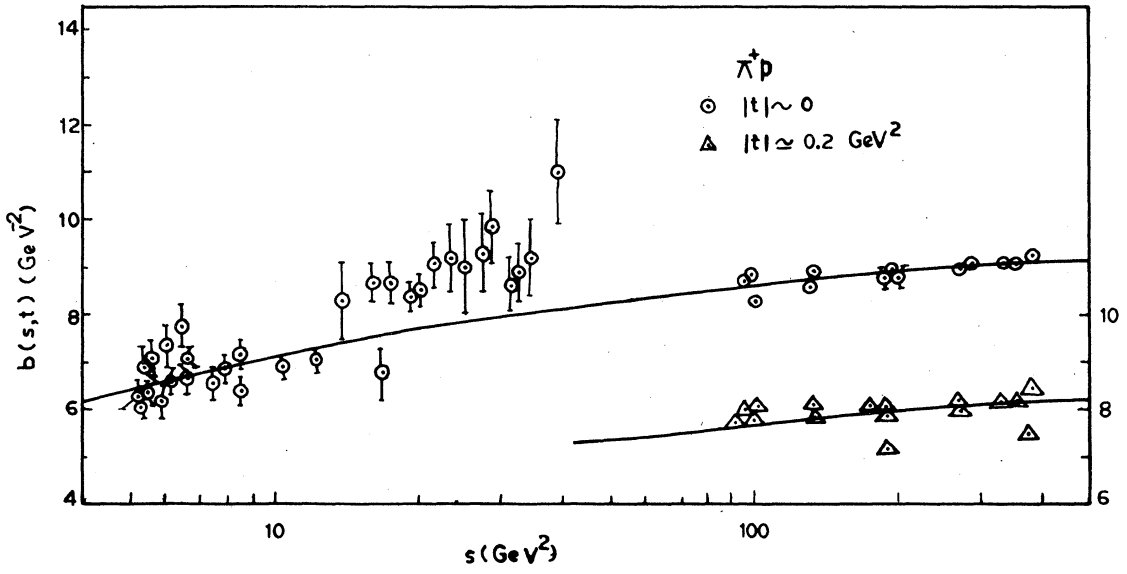

FIG. 9. Fit to the slope-parameter data for π^+p scattering. The circles denote data near forward angles and the triangles denote data for $|t| = 0.2$ GeV^2 for which the vertical scale is shown at the right-hand side of the figure. The solid lines are our fits.

Höhler and Staudenmaier,[35] Krubasik,[35] and Ambats *et al.*,[26] that these data[28] do not join smoothly onto the lower-energy results. In the present analysis we conclude that neither of these data join smoothly onto the higher-energy data[25] also. We suggest that one of the ways to understand this feature is to suppose that the oscillation in the slope parameter observed in the lower-energy region is also present at high energies but with larger period. According to the present fit, the data are consistent with the ~ln$s$ type of asymptotic behavior. The value of λ obtained from data analysis in this case is found to be larger than the theoretical value ($\lambda = m_\pi$) by about 31%. This gives an effective boundary of spectral function which retreats away from the theoretical boundary for energies near threshold. We tried a fit by fixing $\lambda = m_\pi$ and varying all other parameters as given in (27), but found no significant change to the fit of Fig. 9 in the high-energy region, although there was a small change for lower-energy region. However this change does not affect our conclusions on scaling as described subsequently in this section. The fit (27) determines unknown parameters in χ for $\pi^+ p$ scattering. Introduction of other types of asymptotic behaviors either worsened or cound not improve the fit.

(ii) $\pi^- p$ scattering

In this case also, formulas similar to those used for $\pi^+ p$ scattering were used for fitting 48 data points[23,25,26] of forward slopes for $s \geq 4$ GeV^2 and 19 data points[25,26] for the slope parameter at high energies for $|t|_{av} = 0.2$ GeV^2. Although an attempt was made to fit the data with an effective shape[17] for $t_{R_{\pi^- p}}$, the data are found to be consistent with elastic boundary $\lambda = m_\pi$. Thus, best fit in this case is obtained with one parameter less than that for $\pi^+ p$ scattering with

$$d_0 = 0.480\,,$$
$$d_1 = 0.0527\,,$$
$$u_0(s) = 0.312 \text{ GeV}^2\,, \qquad (28)$$
$$C = 1.22\,,$$
$$a = -0.187\,.$$

This yields the χ^2/NDF value 14.4 (12.1) for forward (nonforward) slopes. In this case also, most of the contributions to the χ^2 come from the data of Foley *et al.*[28] in the region $12 \leq s \leq 40$ GeV^2, on which a similar conclusion as that for $\pi^+ p$ scattering has been drawn by the same authors.[35] We note that these data also do not join smoothly to the data at the higher-energy region. One of the possible explanations of such a feature might be due to the presence of oscillations at high energies. In this case also, the fit is consistent with a ~ln$s$ type of asymptotic behavior. For the nonforward data, only one data point contributes 125 to the total χ^2 value of 219. Without this, χ^2/NDF for nonforward slopes is 5.8. The fit (28) has been shown by the solid curves in Fig. 10. It is clear that our fit describes the data reasonably well. The position of the point corresponding to the strong behavior as decided by the value of C is almost the same as in $\pi^+ p$ scattering. Including other types of asymptotic behaviors in the formula either worsened or did not improve the fit.

The values of unknown parameters in χ for $\pi^- p$ scattering are given by (28) and that of $\pi^+ p$ scattering by (27). With the knowledge of χ's for these two processes, we now plot the smaller-angle data[25,26,32] on $f(s,t)$ against the corresponding χ's in Fig. 11. It is clear that the data for these two processes individually and in combination lie on a scaling curve. Figure 12 shows the plot of data for still larger values of $|t|$ in the same energy range. Although data points for high energies are not adequate to exhibit a prominent scaling curve as in the case of pp scattering, there is a clear trend showing that data for larger values of $|t|$ and smaller values of P_{lab} deviate from scaling curve. As energy increases, data for larger values of $|t|$ tend to lie on the scaling curve. In both cases all the data points starting from $P_{lab} = 3$ GeV/c and within $|t| \leq 1.25$ GeV^2 lie on the scaling curve. Data at all available values of $|t|$ with $P_{lab} \geq 50$ GeV/c lie on the scaling curve.

In concluding this section we remark that the use of the s-plane analyticity along with that of the x plane by CPE has improved fits to the slope-parameter data both for forward and nonforward angles. Ambiguity about the possible presence of strong behavior in the interior of figures of convergence for various processes has been clarified. The use of s-plane analyticity has served as a useful tool in getting information on the asymptotic behavior of slope parameters. By using the s-plane analyticity along with that of the x plane, we have been able to demonstrate early on the set of scaling for different elastic diffraction scattering processes in a systematic manner. The results on the asymptotic behavior of slope parameters, the values of C, the maximum value of $|t|$ within which all the data starting from $P_{lab} = 3$ GeV/c scale, and the range of energy investigated for scaling have been summarized in Table I for different processes.

Concerning the results on scaling we find that not only the data for smaller values of $|t|$, but also the data for larger $|t|$ scale in a remarkable manner as demonstrated clearly in the case of pp scattering. Of course the minimum value of P_{lab}

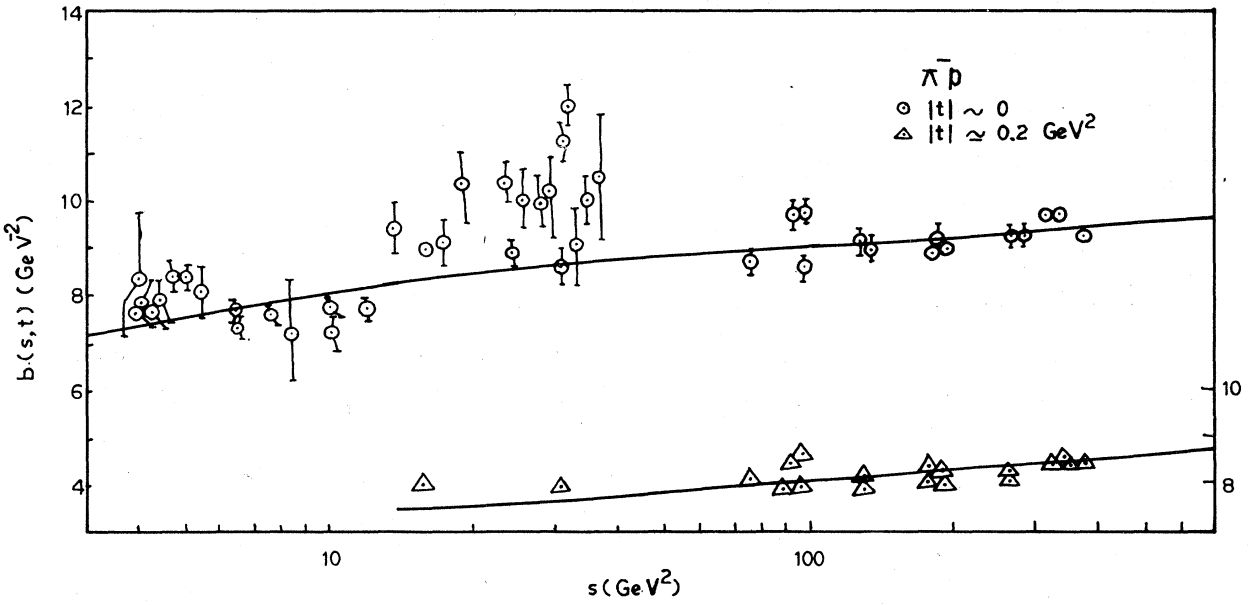

FIG. 10. Fit to the slope-parameter data for $\pi^- p$ scattering. Circles denote data points at forward angles and triangles denote data for $|t| = 0.2$ GeV^2 for which the vertical scale is shown at the right-hand side of the figure. The solid lines are our fits.

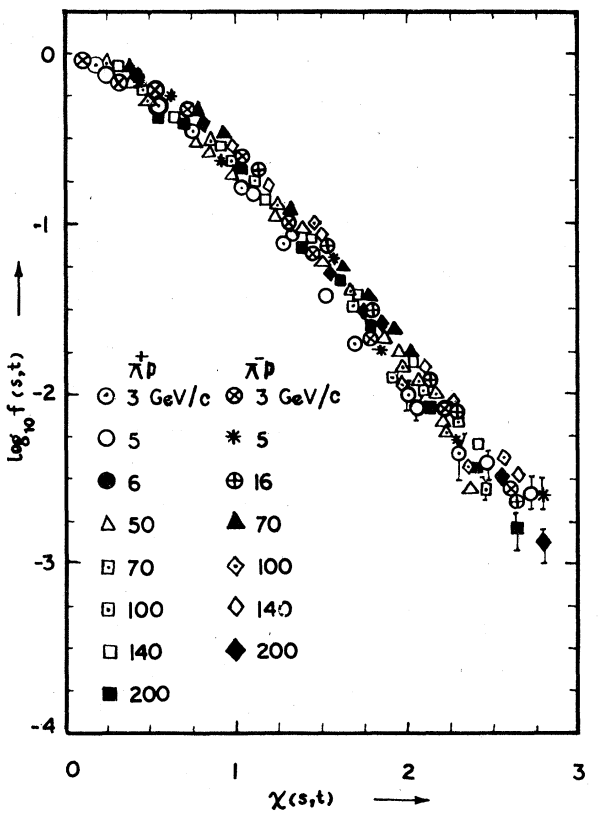

FIG. 11. Scaling and approach to scaling in $\pi^{\pm} p$ scattering.

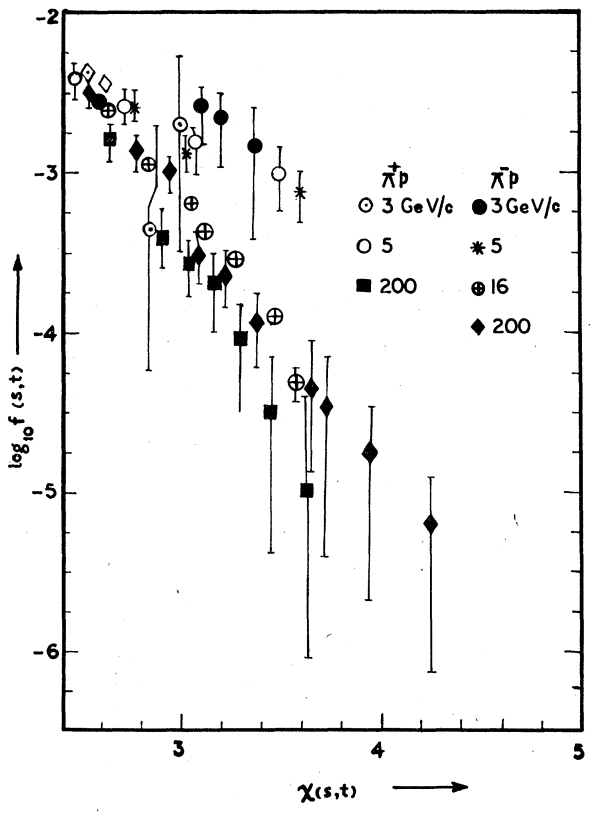

FIG. 12. Scaling and approach to scaling in $\pi^{\pm} p$ scattering for data at larger angles.

TABLE I. Information on the location of strong behavior, asymptotic behavior of the slope parameter, and scaling of cross-section-ratio data for different diffraction scattering processes. For asymptotic behavior the symbol "~" is to be interpreted as "likely to be". $|t|_{max}$ denotes maximum range of $|t|$ of the data for $P_{lab}=3$ GeV/c which lie on the scaling curve. The parameter C with a negative sign gives the position of strong behavior in the x plane.

Process	Value of C	Asymptotic behavior of slope parameter	Range of P_{lab} (GeV/c) investigated for scaling	$\|t\|_{max}$ (GeV^2)
pp	1.913	$\sim(\ln s)^2$	3–1500	1.25
	1.917	$\sim\ln s$		
$\bar{p}p$	1.961	~const	3– 200	0.50
	2.400	$\sim(\ln s)^2$		
K^+p	1.974	$\ln s$	3– 200	2.0
K^-p	1.505	$\sim\ln s$	3– 200	1.0
π^+p	1.211	$\ln s$	3– 200	1.25
π^-p	1.220	$\ln s$	3– 200	1.25

for which scaling starts for larger-$|t|$ data is larger than that for the smaller-$|t|$ data. In particular, the recent data of Akerlof *et al.*[25] and Hartmann *et al.*[29] at $P_{lab}=200$ GeV/c lie almost on the same curve on which the data of De Kerrett *et al.*[29] at $P_{lab}=1500$ GeV/c lie in the scaling plots of Figs. 3(a) and 3(b). To our knowledge there is no other scaling variable in the literature in which scaling of the data has been so systematically exhibited for various processes. It can be argued[10] that the present model has been developed for near forward angles and need not work in representing the data at larger angles. Although there is no convincing explanation yet as to why there is scaling for larger-$|t|$ data, some heuristic plausibility arguments can be put forward, as has been done in Ref. 10. First, the real part may be important for larger angles but the same conformal mapping variable can be used to represent the real part at very high energies at which the domains of analyticity for the real and the imaginary parts are the same if we ignore pole singularities. Second, the short-range forces which possibly influence larger-angle scattering are represented by more distant branch points and by the conformal mapping, although more distant branch point structures have not been explicitly included, their influence is indirectly taken into account by bringing them to closer vicinity of the physical region in the mapped plane. An alternative plausible heuristic explanation may be that the real part effects and influence due to short-range forces are negligible for high energies and at least within $|t|\leq 10$ GeV^2.

IV. RESULTS AND DISCUSSIONS

Use of Mandelstam analyticity of the $x=\cos\theta$ plane alone,[15,16] could not explain high-energy behavior of slope parameters in pp, K^+p, and $\pi^\pm p$ scattering. This deficiency of the proposed formula[16] is ascribed[10] to the lack of inclusion of the s-plane analyticity. Using Mandelstam analyticity of the s plane for the absorptive part of the scattering amplitude along with that of the x plane by conformal mapping, in which the correct physical region in the mapped plane for Laguerre-polynomial expansion is achieved only for asymptotic energies, forward slope-parameter data for pp scattering in all energy ranges could be fitted well,[10] with effective shape of boundary function. However, all the high energy data with $s\geq 35$ GeV^2 could be fitted with theoretical boundary. Experimental data on the pp cross-section ratio starting from $P_{lab}=50$ GeV/c and all available values of $|t|$ appeared to scale against a variable $\chi(s,t)$. But even the data near forward angles for a few GeV/c of the laboratory momentum stayed clearly away from the scaling curve. The onset of scaling from such large values of laboratory momentum may be possibly[10] due to the achievement of the correct physical region only at asymptotic energies and that expansion in Laguerre polynomials is an asymptotic one. This type of conformal mapping and OPE suffers from the deficiency that it cannot explain antishrinkage and shrinkage-antishrinkage pattern of forward peaks at lower energies as observed in the cases of $\bar{p}p$, K^-p, and $\pi^\pm p$ scattering.[17] Further, the conformal mapping used in Ref. 16 for the unsymmetrical cut plane of analyticity develops spurious cuts in the mapped plane which affect convergence of polynomial expansion. This fact has been pointed out in Ref. 10.

In the convergent polynomial expansion (CPE) in terms of the mapped variable z_1, correct physical region has been achieved for all energies.[17] The formula for the slope parameter[17] explains the shrinkage, antishrinkage, and shrinkage-antishrinkage pattern at all energies reasonably well, except for the fact that this formula also fails to account for the observed behavior of slope parameter at asymptotic energies in the cases of pp, K^+p, and π^+p scattering. In this work, analyticity of the s plane for the absorptive part of the scattering amplitude has been used along with the variable z_1 to construct the variable $\chi(s,t)=\alpha(s)z_1$, where $\alpha(s)$ is constructed by conformal mapping

of the s plane and CPE. Unitarity restriction does not allow more than the first two (three) terms in Taylor series in a parabolic (strip) variable. The variable $\chi(s,t)$ has the potentialities of reproducing known scaling variables,[4,7-9] Regge behavior in the amplitude, and providing information about the asymptotic behavior of the slope parameter of the type $\sim(\ln s)^p$ where $p=0,1,2$.

In Ref. 17 only the data on forward slopes were used for the fit and the recently published data.[24,25,26] both for forward and nonforward slopes were not used. Also, efficiency of the formula[17] to fit the nonforward slopes was not tested. In the present work we find that at most the first two terms in the expansion are sufficient to fit the forward slope-parameter data, including the recent data, at all energies and the high-energy slope parameters at $|t|_{av}=0.2$ GeV^2 for pp, $\bar{p}p$, $K^{\pm}p$, and $\pi^{\pm}p$ scattering reasonably well, although only the first term in the expansion is sufficient in the cases of pp and K^+p scattering. The data on K^+p and $\pi^{\pm}p$ scattering are consistent with $\sim\ln s$ type of asymptotic behavior, whereas the data on pp scattering cannot distinguish between $\sim\ln s$ or $\sim(\ln s)^2$ type of asymptotic behavior. Although apparently $\bar{p}p$ and K^-p data support a constant type of asymptotic behavior,[17] the fits to the data are improved by including a formula with $\sim\ln s$ ($\sim(\ln s)^2$) type of asymptotic behavior for K^-p ($\bar{p}p$) scattering. The values of χ^2/NDF for the forward slopes are improved (in some cases very much improved) over that reported in Ref. 17 for all the processes even after including the recent data.[24,25,26] In Ref. 10 an effective boundary of spectral function ρ_{st}, which retreats away from the theoretical one for lower energies, was necessary to fit the slope-parameter data for all energies. However, the data for high energies with $s \geq 35$ GeV^2 could be fitted well with the theoretical elastic boundary. In the present paper the slope-parameter data in all cases have been fitted with the theoretical boundary except for K^-p and π^+p scattering. For K^-p scattering the effective domain of analyticity of the absorptive part used for the fit is smaller, whereas for π^+p scattering it is larger than the theoretical one at lower energies. These are not desirable features according to S-matrix theory, which emphasizes the maximal influence of nearest singularities computed from box graphs.[17] We therefore examined the type of fits obtained with theoretical boundaries. The fits with theoretical boundaries are different from the ones presented here only at lower energies and do not affect our conclusions on the asymptotic behavior of slope parameter and scaling as described in the present paper.

The asymptotic behavior of slope parameters from data analysis is important from the point of view of exact results based upon principles of AFT.[36] Recently Martin[37] has proved that asymptotically the slope parameters for $|t|=0$ for the processes $A+B \to A+B$ and $\bar{A}+B \to \bar{A}+B$ are equal. The analysis of $\pi^{\pm}p$ data supports the same rate of growth for the slope parameters, like $\sim(\ln s)$, for both the processes. There are indications in this analysis that K^-p slope may grow as $\sim\ln s$, the same rate of growth as K^+p scattering, and $\bar{p}p$ slope may grow as $\sim(\ln s)^2$, one of the rates of growths for pp scattering. In none of our analyses have we been able to obtain the equality between particle-particle and antiparticle-particle slopes asymptotically. It may be remembered that errors in the parameters are important before drawing such conclusions. In this analysis, errors in the parameters could not be obtained owing to exigencies in programming in the IBM 1130 Computer. Although the extrapolation of slope parameters to infinity will be carried out in a separate paper, we suppose that data for $s \simeq 1000$ GeV^2 are necessary for $K^{\pm}p$, $\bar{p}p$, and $\pi^{\pm}p$ scattering to verify the asymptotic equality[37] of slope parameters. To determine all the parameters in the formula it has been necessary to fit both the forward and the nonforward slope-parameter data. From the values of the parameter C for different processes, we find that the strong behavior for every process lies outside or on the figure of convergence in the mapped plane for all energies except for the case $s \to s_{th}$ when it may lie in the interior. The distance of the location of strong behavior from the origin in the mapped plane for $\pi^{\pm}p$ scattering is found to be nearer than that in pp, $\bar{p}p$, and $K^{\pm}p$ scattering.

More important is the result of the present work on scaling. The variable $\chi(s,t)$ reduces to the scaling variable[7,8] $tb(s)$ for $s \gg s_{th}$ and $|t| \ll t_R$, and has the potentiality to behave, if unitarity bound is saturated, like the variable[9] $t(\ln s)^2$ in this kinematical region. For $s \gg s_{th}$ and all angles, the variable is like $b(s)z_1$. We note that results[7-9] based upon principles of AFT suggest scaling variables for small $|t|$ and $s \to \infty$, whereas $\chi(s,t)$ reduces to the variables for $s \gg s_{th}$, which condition can be achieved much earlier than the limit $s \to \infty$. The variable χ, however, contains unknown parameters which are determined by fitting the slope-parameter data as described above. When the cross-section-ratio data for different processes are plotted against the corresponding χ's, all the available data for every process starting from $P_{lab}=3$ GeV/c and for $|t| \leq |t|_{max}$, where $|t|_{max}$ in general varies from process to process, lie on a separate scaling curve. As the energy increases from $P_{lab}=3$ GeV/c, data for values of $|t|$ larger than $|t|_{max}$, for every process and any fixed energy,

lie on the corresponding scaling curve. Cross-section-ratio data for all available values of $|t|$ and for $P_{\text{lab}} \geq 50$ GeV/c lie on the corresponding scaling curve for every process. The values of $|t|_{\max}$ are 1.25, 0.50, 2.0, 1.0, and 1.25 GeV^2 for pp, $\bar{p}p$, K^+p, K^-p, and $\pi^\pm p$ scattering, respectively. Although the scaling variable χ is different for different processes and scaling curves for pp and $\bar{p}p$ appear to be different, scaling curves for π^+p and π^-p scattering appear to be the same. The scaling curves for K^+p and K^-p scattering appear to be almost the same. Our scaling for every process appears to be better than all other existing plots, particularly those of geometrical scaling[2,3,30] in the variable $t\sigma_{\text{tot}}$ and that of Divakaran and Gangal[6] in the variable $t\sigma_{\text{tot}}{}^2/\sigma_{\text{el}}$, and almost the same as that of Hansen and Krisch[2] in the variable $ut\,\sigma_{\text{tot}}(s)/[s\sigma_{\text{tot}}(s)]$ for pp scattering at small t, but better than these for data at larger $|t|$ values. Particularly in the case of pp scattering, the energy dependence for data within $|t| \leq 1.25$ GeV^2 has been very effectively removed, more effectively than what has been done in Ref. 10. As in Ref. 10, the present variable χ proves to be a remarkably good scaling variable even for high-energy data for larger values of $|t|$ lying well outside the diffraction peak region. In particular, recent data for pp scattering at all available values of $|t|$ and $P_{\text{lab}} = 200$ GeV/c and 1500 GeV/c lie on the same curve. This is evident from Figs. 3(a) and 3(b). The scaling of the $\pi^\pm p$, and $\bar{p}p$ scattering appear to be similar. Although scaling of the K^+p and K^-p scattering cross-section-ratio data are individually similar to that of pp scattering, there is a spread in the scaling curve in Fig. 7 where the individual processes have been plotted together. Results based on AFT predict scaling only in the asymptotic energy region and within the diffraction peak $|t| < 4m_\pi{}^2$. In this analysis, scaling in the variable χ has been achieved much earlier in the energy scale and for much larger values of $|t|$. The possible main reasons for the early onset of scaling might be due to the achievement of the correct physical region for all energies and the possibility that χ reduces to the known scaling variables earlier in energy scale than the limit $s \to \infty$. Other possible reasons may be the special weight given to the right-hand cut as compared to the left-hand cut and the additional convergence of CPE in the kinematical region for which $|t| \ll t_R$ and $|4q^2 + t_L - \Delta/s| \gg |t|$. In Ref. 10 it was found that expansion in terms of Laguerre polynomials in the mapped variable z is an asymptotic expansion. At finite energies, however, convergent expansion was possible for any finite energies with orthogonal polynomial whose nature and the convergence of the series vary with energy. But OPE was shown to be an asymptotic property. In the present case, CPE in terms of Laguerre polynomials in the variable z_1 is possible for all energies where the convergence of the series for any particular process increases with energy. However, again in this case, OPE is achieved only at asymptotic energies.

Auberson, Kinoshita, and Martin[4] have shown that the amplitude ratio for the absorptive part becomes an entire function of their scaling variable for $s \to \infty$ within the diffraction peak. In the present case we find from Table I that there are indications for every slope parameter to grow like $\sim \ln s$ or $\sim (\ln s)^2$ for $s \to \infty$. Thus, in the plane of the variable $\chi(s,t) = \alpha(s) z_1$, the images of the cuts move away to infinity for $s \to \infty$, but the physical region is still the right half of the real axis $0 \leq \text{Re}\chi \leq \infty$. Thus, in our analysis also there is evidence that the domain of analyticity in some or all of the diffraction scattering processes may be the entire χ plane minus the points at infinity when $s \to \infty$. In this limit the image of the cuts coincide with the limiting parabola whose interior is the image of the entire domain of analyticity of the x plane and CPE becomes OPE. It might then be possible that the same number of terms with the same coefficients represent the data for different energies in the asymptotic energy region. Our data analysis on scaling suggests such a possibility and that scaling starts earlier in the energy scale for the data near forward angles. Cornille[8] has defined a class of scaling functions in which are included series in orthogonal polynomials including Laguerre, but excluding Hermite polynomials. In the present case we find that a series in Laguerre polynomials in the variable χ is a good candidate for scaling function. In this paper no attempt has been made to find out scaling function. The scaling function can be determined by fitting the cross-section-ratio data in the scaling region covering a wider angular range for any energy after $P_{\text{lab}} = 50$ GeV/c. Then the CPE (8), with the coefficients e_n's determined by this data fitting represents scaling function. This work will be carried out and reported in a future paper.

Finally, we summarize limitations and possible flaws in the representation developed here. Some of the limitations are common to this paper and Ref. 10. Here only the cut contributions of the absorptive part of the amplitude have been used to develope a representation for the differential cross section and the contribution due to poles has been neglected. It is well known that poles lying on the real axis contribute to the real part. There are many works[4-9] in the literature which neglect pole contributions. It has been shown by Singh and Roy[5] by model-independent analysis that the unitarity

upper bound of the absorptive part of the amplitude saturates the high-energy data near forward angles for πN and pp scattering.[5,19] Experimental measurements at high energies show that the real part of the amplitude is small near forward angles for NN, πN, and KN scattering. But away from the forward direction, interference between pole and the Pomeron (cut) contribution may be substantial, thus contributing to the slope. In the present paper, pole contribution for nonforward angles has not been included. But it is apparent that the explicit introduction of pole contribution will spoil simple realization of scaling, as has been described in this paper. Second, the rate of convergence of the series expansion in terms of Laguerre polynomials is not unique with respect to energy. For any particular process, the convergence of the series increases with energy reaching its maximum only at asymptotic energy. Third, it can be argued that the present model has been developed for scattering near the forward angles and need not work in representing large-angle data. But actually, at very high energies, scaling of the larger-angle data lying well outside the diffraction peak region is observed to be occurring for pp scattering. There is no convincing explanation yet as to why such a thing occurs in the present model, although some heuristic (plausibility) arguments may be put forward, as has been done in Sec. III and in Ref. 10: It is possible that at high energies, if one neglects the pole contribution, the same parabolic variable can represent the real part also, because at these energies the distinction between the domains of analyticity drops out. Further, the possible influence of short-range forces for large-angle scattering, which are represented by more distant branch points, has been indirectly taken into account by conformal mapping that brings the position of such branch points to closer vicinity of the physical region in the mapped plane. Alternative plausibility arguments may be that real part effects and/or the influence of short-range forces may be negligible even at the large range of $|t|$ used in this paper. Fourth, a limitation of a serious nature arises when conformal mapping of the type described earlier[16] and in Ref. 10 are used for the unsymmetrical cut x plane of analyticity. In that case,[10] spurious cuts occur inside the figure of convergence in the mapped plane which do affect CPE or OPE. In the present case also, the square transformation involved in $g(x)$ introduces spurious branch points at $z_1 = 0$ ($\chi = 0$) and $z_1 = \infty$ ($\chi = \infty$), giving rise to a spurious cut completely overlapping the image of the physical region in the $z_1(\chi)$ plane. Regarded as an analytic function of x, the conformal transformation z_1 does not introduce extra branch points except those obtained from dynamics for all cases except for pp scattering. Therefore, the representation does not violate analyticity for any other process except for pp scattering. It may be questioned whether the spurious cut affects convergence of polynomial expansion in the mapped plane. At present we do not have any clear answer to such a question but provide examples of analyses where branch cuts of a more serious nature are present. In the work of Ciulli,[12] results on the convergence of polynomial expansion have been taken to hold true in the presence of an artificial cut present in the interior of the figure of convergence covering the entire physical region. Barrelet[38] has used the theory of analytic approximations with conformal transformation, which introduces cuts explicitly in the physical region. In the presence of the spurious cut lying on the physical region, the convergence of polynomial expansion perhaps holds true for physical values of the variable with $\mathrm{Re}z_1 \pm i\epsilon$ or $\mathrm{Re}\chi \pm i\epsilon$ prescriptions, above or below the spurious cuts. Therefore, we suppose that such a spurious cut may not cause any trouble for convergence so long as its presence is confined to the image of the physical region only in the mapped plane. A serious objectionable feature which occurs for pp scattering only is due to the introduction of Krisch[1] type of line of zero into conformal mapping. Such a line of zero introduces spurious branch points in the s plane as discussed in Sec. III and violates the analyticity property of the amplitude. Since the parameter a is negative for this line of zero, the images of these branch points lie on the $\mathrm{Im}\zeta$ ($\mathrm{Im}\eta$) axis. The convergence of Taylor series in ζ (η) is, therefore, limited due to their presence. In spite of this flaw, we have used Krisch type of line of zero in the absence of any other definite line of zero for pp scattering and for the sake of simplicity since it contains no other free parameters.

Our formula for slope parameter has not provided an adequate explanation for the oscillatory pattern of slope parameters in the lower-energy region in the case of $\pi^{\pm} p$ scattering, for which it describes only the average of the data, and $K^- p$ scattering, for which oscillations have not been fully described. Such lower energies do not enter into the scaling region as described here. In the case of $\pi^- p$ scattering, the oscillatory pattern near threshold energies has been described[17] using a curved line of zero. It has been speculated[17] that the inclusion of complex zero trajectories[38,39] into the formula may explain observed oscillations. Such a conjecture has been found to be true recently, at least in the case of $\pi^- p$ scattering.[40]

The scaling in the variable of Krisch type[1,2] has

been hypothesized and geometrical scaling has been assumed by Dias de Deus.[3] In these cases, of course, the hypothesis or assumption has been supported by physical arguments. Scaling in the variables[4-9] obtained from the principles laid down by AFT are based upon more rigorous mathematical foundations; scaling in the variable of Ref. 10 and in the present work is not proved *a priori* but hypothesized from considerations of uniqueness of OPE at asymptotic energies in the context of parabolic transformation. Experimental data on cross-section ratios have been used to justify such a hypothesis. As has been remarked in Ref. 17, experimental data are always not enough to justify the representations used. Clearly, many other representations using different types of conformal transformations may be possible. Nevertheless, our investigation provides a global understanding of diffraction scattering.

ACKNOWLEDGMENT

The author expresses his gratitude to Professor Trilochan Pradhan for providing facilities at the Institute of Physics, Bhubaneswar where most of this work was done. He expresses his gratitude to Professor B. M. Udgaonkar for encouragement and to Dr. S. M. Roy for valuable comments. Financial assistance from the University Grants Commission in the form of a National Associateship Scheme and computation facility from the Computer Centre, Utkal University are thankfully acknowledged.

---

*Present address.
[1]A. D. Krisch, Phys. Rev. Lett. 19, 1149 (1967); A. D. Krisch, Phys. Lett. 44, 71 (1973); E. Leader and M. R. Pennington, Phys. Rev. D 7, 2668 (1973).
[2]P. H. Hansen and A. D. Krisch, Phys. Rev. D 15, 3287 (1977).
[3]J. Dias de Deus, Nucl. Phys. B 59, 231 (1973); A. J. Buras and J. Dias de Deus, *ibid.* B 75, 981 (1974); J. Dias de Deus, Rutherford High Energy Physics Laboratory Report No. RL-75-125 (T-132), talk delivered at the XVth Zakopane Summer School, Poland, 1975 (unpublished).
[4]G. Auberson, T. Kinoshita, and A. Martin, Phys. Rev. D 3, 3185 (1971).
[5]V. Singh and S. M. Roy, Phys. Rev. Lett. 24, 28 (1970); Phys. Rev. D 1, 2638 (1970).
[6]P. P. Divakaran and A. D. Gangal, Nucl. Phys. B 114, 100 (1976).
[7]H. Cornille and A. Martin, CERN Report No. TH 2130, (1976) (unpublished); talk presented by A. Martin at the Orbis Scientae, Coral Gables (unpublished).
[8]H. Cornille, Phys. Rev. D 14, 1693 (1976).
[9]G. Auberson and S. M. Roy, Nucl. Phys. B 117, 322 (1976).
[10]M. K. Parida, preceding paper, Phys. Rev. D 19, 150 (1979). Hereafter we refer to this paper as I.
[11]F. Cerrulus and A. Martin, Phys. Lett. 8, 80 (1964); A. Martin, Nuovo Cimento 37, 671 (1965).
[12]R. E. Cutkosky and B. B. Deo, Phys. Rev. 174, 1859 (1968); S. Ciulli, Nuovo Cimento 61A, 787 (1969).
[13]S. Ciulli, Phys. Rep., 17C, 133 (1975).
[14]Y. A. Chao, Phys. Rev. Lett. 25, 309 (1970); R. E. Cutkosky and B. B. Deo, Phys. Rev. D 1, 2547 (1970); R. C. Miller, T. B. Novey, A. Yokosawa, R. E. Cutkosky, H. R. Hicks, R. L. Kelley, C. C. Shih, and G. Burleson, Nucl. Phys. B37, 401 (1972).
[15]B. B. Deo and M. K. Parida, Phys. Rev. Lett. 26, 1609 (1971).
[16]B. B. Deo and M. K. Parida, Phys. Rev. D 8, 249 (1973).
[17]M. K. Parida, Phys. Ref. D 17, 785 (1978).
[18]B. B. Deo and M. K. Parida, Phys. Rev. D 8, 2939 (1973); 2068 (1974).
[19]F. Halzen, in *Particle Interactions at Very High Energies*, proceedings of the 2nd Louvain Summer Institute on Particle Interactions at Very High Energies: Duality in Elementary Particle Physics, 1973, edited by D. Speiser *et al.* (Plenum, New York, 1974).
[20]R. E. Cutkosky, Carnegie Mellon University Report No. COO-3066-2, 1972 (unpublished).
[21]B. B. Deo, Phys. Rev. D 9, 3513 (1974).
[22]S. M. Roy, Phys. Rep. 5C, 125 (1972); H. Cornille and A. Martin, Nucl. Phys. B37, 1 (1973). See also Ref. 9.
[23]T. Lassinski, R. Levisette, B. Schwarzschild, and P. Ukleja, Nucl. Phys. B37, 1 (1972).
[24]G. G. Beznogikh *et al.*, Phys. Lett. 30B, 274 (1969); M. Holder *et al.*, *ibid.* 35B, 355 (1971); U. Amaldi *et al.*, *ibid.* 36B, 504 (1971); 44B, 116 (1973); 66B, 390 (1970); G. Barbiellini *et al.*, *ibid.* 39B, 663 (1972); V. Bartenev *et al.*, Phys. Rev. Lett. 31, 1088 (1973); 31, 1367 (1973); Kh. M. Chernev *et al.*, Phys. Lett. 36B, 266 (1971); P. Jenni *et al.*, Nucl. Phys. B129, 232 (1977).
[25]C. W. Akerlof *et al.*, Phys. Rev. Lett. 35, 1406 (1975); Phys. Rev. D 14, 2864 (1976); Fermilab Single Arm Spectrometer Group, Phys. Rev. Lett. 35, 1195 (1975); D. S. Ayres *et al.*, Phys. Rev. D 15, 3105 (1977).
[26]I. Ambats *et al.*, Phys. Rev. D 9, 1179 (1974).
[27]R. Odorico, Nucl. Phys. B37, 509 (1972).
[28]K. J. Foley *et al.*, Phys. Rev. Lett. 11, 503 (1963); K. J. Foley *et al.*, Phys. Rev. 181, 1775 (1969).
[29]J. V. Allaby *et al.*, Phys. Lett. 28B, 67 (1969); A. A. Bohm *et al.*, *ibid.* 49B, 491 (1974); N. Kwak *et al.*, *ibid.* 49B, 491 (1974); N. Kwak *et al.*, *ibid.* 58B, 233 (1975); G. Barbiellini *et al.*, *ibid* 39B, 663 (1972); H. De Kerret *et al.*, *ibid.* 62B, 363 (1976); 68B, 374 (1977); J. L. Hartmann *et al.*, Phys. *Rev.* Lett. 39, 975 (1977).
[30]G. Giacomelli, Phys. Rep. 23C, 125 (1976).

[31]Y. Antipov *et al.*, Nucl. Phys. B37, 333 (1973); P. Jenni *et al.*, *ibid.* B129, 232 (1977).
[32]J. S. Russ *et al.*, Phys. Rev. D 15, 3139 (1977).
[33]V. Barger and D. Cline, Nucl. Phys. 23B, 227 (1970).
[34]T. J. Weare, Nuovo Cimento 9A, 173 (1972).
[35]G. Höhler and H. M. Staudenmaier, University of Karlsruhe report, 1972 (unpublished); E. Krubasik, Nucl. Phys. B44, 558 (1972).
[36]V. Singh, private communications.
[37]A. Martin, in *New Phenomena in Subnuclear Physics*, edited by A. Zichichi (Academic New York, 1975).
[38]E. Barrelet, Nuovo Cimento 8A, 331 (1972).
[39]A. A. Carter, J. Phys. G 3, 1215 (1977).
[40]M. K. Parida and B. P. Mahapatra (unpublished).